UNIVERSITY OF LEEDS

Dr. Elena Maters
School of Earth and Environment
University of Leeds
Woodhouse Lane
Leeds, LS2 9JT
United Kingdom
e.c.maters@leeds.ac.uk

24 March 2019

Dear Dr. Ryan Sullivan,

Thank you for your handling of our manuscript entitled "The importance of crystalline phases in ice nucleation by volcanic ash" (acp-2018-1326) in consideration for publication as a Research Article in *Atmospheric Chemistry and Physics*.

Following up on your request for revisions, we present for your evaluation a detailed reply to the Reviewer comments, as well as a carefully revised manuscript. We have been able to respond fully to all comments and have integrated suggestions to improve the manuscript, or else have explained why they may not be applicable within the context of our study.

The Reviewers express interest in the novelty of our study and confidence in the quality of the data as well as its contribution to the state of knowledge. The main requests related to better placing our work in the context of previous works and acknowledging other interpretations of our results for instance regarding the potential role of pyroxene in nucleating ice. We have now inserted more background on studies of ice nucleation by volcanic ash in the Introduction, and have addressed a very recent study reporting the importance of feldspar and pyroxene in ice nucleation by volcanic ash in the Discussion. We have also revised wording in several places to ensure that plagioclase feldspar and pyroxene are both conveyed as plausible agents responsible for the ice-nucleating activity of the tephra samples that lack alkali feldspar. We recognise that some of our interpretations are speculative and we reiterate that additional studies will be needed to unravel the precise role of mineralogy in ice nucleation by volcanic ash, for example using a combination of pure mineral samples and optical and microanalytical techniques to investigate ice nucleation on a range of solid surfaces relevant to ash.

The other comparatively minor queries raised by the Reviewers have been fully addressed in our reply and/or translated into clarifications in the manuscript or supplement text where necessary.

We thank you for your time and hope that this new submission meets with your approval. We look forward to hearing from you.

Yours sincerely,

Elena Maters

Authors' response to Reviewers' comments on "The importance of crystalline phases in ice nucleation by volcanic ash" (acp-2018-1326)

We thank the two Reviewers for their helpful evaluation of our manuscript. We have been able to respond to all comments and provide a carefully revised manuscript. The comments in italic and our responses in normal type are given below. Examples of relevant text (existing or new) are presented in grey highlight between quotation marks. The line numbers that we refer to correspond to those in the revised manuscript.

REVIEWER #1

Major Comments

The title of the paper emphasizes the importance of crystalline phases. This, while qualitatively true, is poorly supported by the quantitative techniques in this paper. For example, the LIPteph, LIPglass, CIDteph, and CIDglass are all devoid of crystalline material (<2%, i.e., below the limit-of-detection of the instrument), yet they all have vastly different ice nucleation abilities. In addition, their "glass" examples generally differ from their "teph" case. These are two of the nine cases, so they are over 20% of the samples. Ultimately, that some ice active mineral components (or at least 1400-1600 C labile components) that are present at less than 2% is an interesting result from this work that needs further highlighting.

We agree with the Reviewer that differences in INA between LIP_{teph}, LIP_{glass}, CID_{teph}, and CID_{glass}, which all have <2 wt.% crystalline material, should be addressed given our emphasis of the importance of crystalline phases.

We acknowledge already on Page 4 Lines 8-10 that "While the LIP_{teph} and CID_{teph} crystallinities cannot be quantified below the ~2 wt.% limit of the technique, this does not rule out the possibility of smaller amounts of crystals and/or nanoscale crystallites being present in these samples." Table 2 lists crystalline phases that might occur as minor components below quantification in the tephra, including Fe(-Ti) oxide in LIP_{teph}, and alkali feldspar, clinopyroxene, and Fe(-Ti) oxide in CID_{teph}. These minor components could be why the two dominantly glassy tephra samples show different INA and are still more ice-active than their counterpart glass samples (Figure 3a,d). We have inserted text in the discussion to highlight this:

Page 5 Lines 33-35: "Even the dominantly glassy LIP_{teph} and CID_{teph} (<2 wt.% crystallinity) display higher INA than their counterpart LIP_{glass} and CID_{glass}, which could reflect the influence of minor crystalline components (below quantification by XRD; Table 2) in these tephra on their ability to nucleate ice."

The observation that CID_{teph} is only slightly more ice-active than CID_{glass} (Figure 3d) may, as the Reviewer suggests, reflect some ice-active mineral components also present in amounts <2 wt.% in this glass sample following melting, homogenising, and quenching. This possibility is supported by the observation that CID_{glass} nucleates ice at warmer temperatures than the background water and the other glass samples (Figure 2b,d). We have inserted text in the discussion to highlight this also:

Page 8 Lines 26-28: "It is possible that CID_{glass} and COL_{glass} contain very small amounts of crystals below detection by XRD that survived melting or formed during quenching, which could explain why these glasses stand out in their ability to nucleate ice."

Overall, we think that our findings, both quantitative and qualitative, support the title of the paper.

Page, 5, Line 26: In this work alone, there is much evidence that Na/Ca-feldspar is not responsible for ice nucleation. For example, the plagioclase parameterizations from Harrison et al. (in prep) are much too low to explain the ice nucleation efficiency of almost all of the ash samples in this work, regardless of their plagioclase content. Furthermore, while Harrison et al., 2016 have shown that higher Na2O/CaO may imply higher ice nucleation activity for some feldspars, Page 5, Line 40 is direct contrast to previous studies that have shown that very pure albite is not that ice nucleation active [e.g., Zolles et al., 2015, Schill et al., 2015,

Welti et al., 2019]. Alternatively, while there is less literature evidence that orthopyroxene may be the responsible agent, it seems like a much more feasible choice here. It is interesting to the reviewer that the authors then suggest in the conclusion that intermediate to felsic alkaline magmas may then have a higher propensity to contain ice-active ash in their eruptions.

We acknowledge that we can improve the presentation of our arguments in this section. The Reviewer is correct that the high INA of tephra samples containing plagioclase feldspar (Page 6 Lines 34-35) "are inconsistent with the relatively low INA of Na-/Ca-feldspar reported in the literature (Fig. 5)." However, evidence of exceptionally ice-active feldspars including a hyper-active Na-feldspar (Amelia albite; characterised by the plagioclase structure) has been presented by Harrison et al. (2016), which we mention and now plot in Figure 5 to illustrate that highly ice-active plagioclase feldspar exists in nature. Even excluding this hyper-active albite, and contrary to the Reviewer's remark that "***albite is not that ice nucleation active***", a new Na-feldspar parameterisation compiled from literature data (Harrison et al., in prep.), which we have also added to Figure 5, falls much closer to the high INA shown by COL_{teph} and TUN_{teph} (Fig. R1 below). We have revised the text as follows:

Page 6 Lines 35-40/Page 7 Lines 1-4: "This may point to the presence in COL_{teph} and TUN_{teph} of ice-active plagioclase feldspar characterised by an INA closer to the Na-feldspar (albite) parameterisation, or potentially more akin to the hyper-active feldspars measured by Harrison et al. (2016; Fig. 5). It is not clear why these hyper-active samples (Amelia albite and TUD#3 microcline) have a much greater INA relative to the majority of feldspars tested (Harrison et al., 2016; Peckhaus et al., 2016), but such wide variability may relate to the specific mechanisms and/or conditions of formation and subsequent processing of individual samples (Welti et al., 2019), and it might be that plagioclase feldspar in COL_{teph} and TUN_{teph} was produced in a way that gives rise to enhanced activity."

Together, the three parameterisations and two hyper-active samples clearly demonstrate the wide variability in INA of feldspar minerals investigated to date. In light of this variability, we maintain our suggestion that highly ice-active plagioclase feldspar might occur in COL_{teph} and TUN_{teph}.

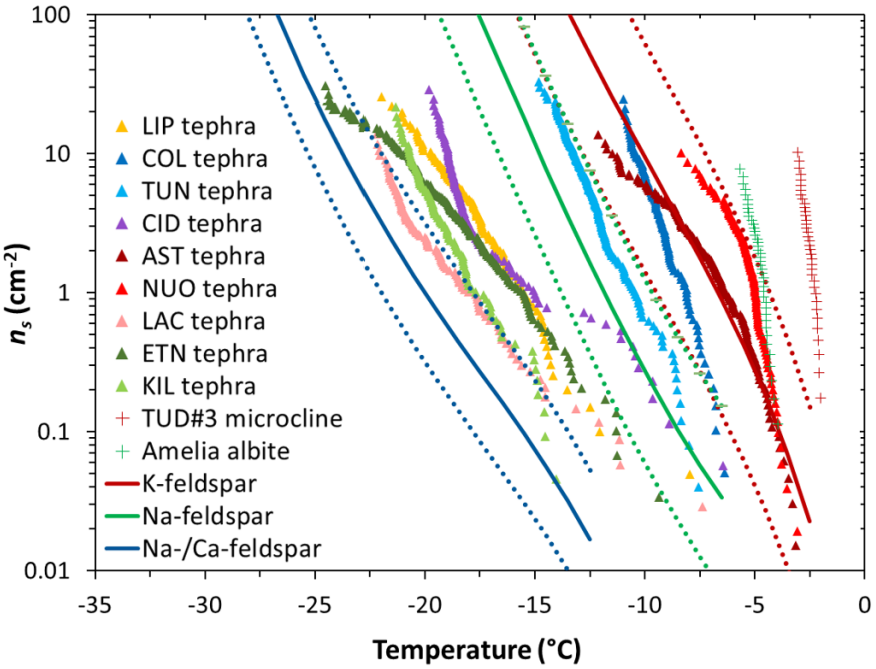

Figure R1. Ice nucleation active site density (n_s) as a function of temperature for 1 wt.% suspensions of tephra in water. The red and green crosses are the $n_s(T)$ values for, respectively, a hyper-active K-feldspar (TUD#3 microcline) and a hyper-active Na-feldspar (Amelia albite) measured by Harrison et al. (2016). The red, green, and blue lines represent parameterisations for, respectively, K-feldspar, Na-feldspar, and Na-/Ca-feldspar reported in Harrison et al. (in prep.) from a compilation of literature data, excluding the hyper-active feldspar specimens. The solid lines indicate mean values and the dashed lines indicate lower and upper limits corresponding to the standard deviation of the mean.

We understand the Reviewer's sentiment "***that orthopyroxene may be the responsible agent***" and we acknowledge (Page 7 Lines 4-5) that the high INA of COL_{teph} and TUN_{teph} alternatively "may relate to the influence of some other mineral component such as orthopyroxene" on ice nucleation by these samples. However, as the Reviewer points out, there is limited literature on ice nucleation by pyroxenes, and so we conclude (Page 8 Lines 11-13) that "we cannot rule out a potential influence of pyroxene on ice nucleation by volcanic ash" and "additional research is needed to quantify the INA of a range of pyroxene minerals, and probe the nature of their ice-nucleating properties, in order to better inform this assessment." We have additionally highlighted a very recent study on ice nucleation by volcanic ash and pyroxene in our discussion:

Page 6 Lines 22-23: "More recently, Jahn et al. (2019) proposed that feldspar and pyroxene were responsible for ice nucleation by ash from Soufrière Hills, Fuego, and Santiaguito volcanoes."

Page 8 Lines 6-11: "More recently, Jahn et al. (2019) measured the INA of a clinopyroxene specimen (freezing from -8 to -24 °C), citing its behaviour to explain the INA of three pyroxene-containing volcanic ash samples. However, XRD analysis indicated that this specimen comprising diopside-augite also contained ~5 wt.% feldspar, which might have influenced the INA observed. In any case, it should be emphasised that a single mineral specimen might not provide a good representation of the INA of a given mineral type, as shown by studies on ice nucleation by feldspar and quartz (Harrison et al., 2016; Whale et al., 2017; Harrison et al., in prep.)."

Our own measurements of a range of pyroxene samples (wollastonite, diopside, augite, enstatite, hypersthene) do not show these minerals to be especially ice-active (Maters et al., in prep.). Therefore, we do not agree that orthopyroxene "***seems like a much more feasible choice***" to explain the high INA of COL_{teph} and TUN_{teph} in our study. However, we recognise that some content in our original manuscript conveyed a preference for the hypothesis of ice-active plagioclase feldspar over that of ice-active orthopyroxene. In light of the Reviewer's comments, and given that we currently lack enough information to conclude definitively which may be the most ice-active mineral(s) in the studied tephra (specifically COL_{teph} and TUN_{teph}), we have modified this content so as not to favour either hypothesis:

Page 1 Lines 17-19: "There is evidence of a potential indirect relationship between chemical composition and ash INA, whereby a magma of felsic to intermediate composition may generate ash containing highly ice-active feldspar or pyroxene minerals."

Page 6 Lines 26-28: "[…] while the next most ice-active COL_{teph} and TUN_{teph} are characterised by an abundance of plagioclase feldspar (55 and 43 wt.%, respectively; Fig. 4b) and lesser amounts of orthopyroxene (7 and 5 wt.%, respectively, Fig. 4d)."

Page 8 Lines 33-35: "[…] the $T_{n_s \approx 1\ cm^{-2}}$ decreases with increasing Fe_2O_3, MgO, and CaO contents for NUO_{teph}, AST_{teph}, COL_{teph}, TUN_{teph}, ETN_{teph}, and KIL_{teph} (Fig. 6), in an order consistent with interpretations relating to their feldspar contents and chemistries and/or a potential effect of orthopyroxene in two of these samples (see discussion Sect. 4.2)."

Page 9 Lines 17-20: "[…] we speculate that highly ice-active ash particles might be erupted by volcanoes with intermediate to felsic alkaline magmas giving rise to feldspar crystals featuring overgrowth textures (e.g., Astbury et al., 2016; 2018) or potentially pyroxene crystals with high INA for reasons yet unknown (e.g., Jahn et al., 2019)."

Figure 6: We have inserted the orthopyroxene content of COL_{teph} and TUN_{teph} in the legend.

Lastly, the Reviewer implies that the possibility that (ortho)pyroxene is highly ice-active contradicts our concluding speculation (Page 9 Lines 17-20) that intermediate to felsic alkaline magmas might give rise to highly ice-active ash, presumably because pyroxene can also form in mafic magmas (Figure 1a). However, this

speculation is borne from observations that the most ice-active samples (COL_{teph}, TUN_{teph}, NUO_{teph}, AST_{teph}) are those originating from intermediate to felsic magmas (Figure 6), and is not fundamentally affected by whether it is the (ortho)pyroxene, plagioclase feldspar, or alkali feldspar driving ice nucleation by these samples. In contrast, no empirical evidence leads us to speculate that mafic magmas might give rise to highly ice-active ash, as the much less ice-active samples (ETN_{teph}, KIL_{teph}) containing (clino)pyroxene and/or plagioclase feldspar are those originating from mafic magma (Figure 6). We infer (Page 7 Lines 8-9) that even when tephra samples contain common minerals, "differences [in INA] might relate to the specific chemistry of the mineral phases present in the tephra (Zolles et al., 2015; Welti et al., 2019)," which likely varies depending on factors including magma composition. We thus stand by our original suggestion that intermediate to felsic magmas might erupt highly ice-active crystalline ash.

Page 6, Line 1. The electron microprobe studies are not described in the text or in the supplemental. I see from Text S1 that the spot size is ~10 um; however, it would be useful to know some quantitative limits on this technique as well as how many spot sizes per sample were looked at.

The electron microprobe analysis is described in the Supplementary Material, specifically in Text S1, which is referred to by the Reviewer. We have added details regarding the number of spots analysed as well as quantitative limits on this technique:

Supplement Page 3 Lines 2-5: "A 10 µm focused beam was used at an accelerating voltage of 15 keV and a current of 5 nA to analyse at least five points for each crystalline phase in the tephra samples. Elemental detection limits in parts per million are as follows: Si - 786, Al - 655, Fe - 1573, Mg - 501, Ca - 747, Na - 973, K - 711, Ti - 894, Mn - 1401, P - 568, Cr - 1286, S - 767, Cl - 955."

Page 6, Line 9. I am confused by this paragraph. The authors spend a great deal of time describing why LACteph does not have perthitic intergrowth microtexture, but then end the discussion by stating that NUOteph and ASTteph also don't have perthitic intergrowth microtexture. This seems like a logical fallacy to me. A similar sentiment is felt for the section on the anti-rapakivi texture. Was it not observed in the LACteph sample? Finally, how are all of these these surfaces susceptible to changes upon milling with a zirconia ball and vial?

We have revised the text in this paragraph to improve our reasoning and have added reference to a very recent study of ice nucleation by various K-feldspars (Welti et al., 2019):

Page 7 Lines 22-39: "However, perthite in alkali feldspar develops in metamorphic and plutonic contexts during slow cooling at temperatures <700 °C (Parsons, 2010), and is generally not expected in volcanic ash which cools rapidly from magmatic down to ambient temperatures during explosive eruption (Parsons et al., 2015). An absence of perthitic microtexture is consistent with the low INA of LAC_{teph} in spite of its alkali feldspar content (9 wt.%). This is supported by evidence that the alkali feldspar mineral sanidine sourced from the same geological setting as LAC_{teph} (Eifel volcanic field) lacks perthitic texture and exhibits a poor ability to nucleate ice (Whale et al., 2017). A recent study similarly found volcanic sanidine from Germany to be the least ice-active among the alkali feldspar samples tested (Welti et al., 2019). In contrast, an absence of perthitic microtexture is inconsistent with the high INA of NUO_{teph} and AST_{teph}, and perhaps some other textural feature underlies these samples' ability to nucleate ice as effectively as alkali feldspar of non-pyroclastic origin (Fig. 5). Pyroclastic material from both the 1538 Monte Nuovo eruption (i.e., the origin of NUO_{teph}) and the ~4 ka Astroni eruption (i.e., the origin of AST_{teph}) has been found to contain anti-rapakivi overgrowth microtexture characterised by plagioclase feldspar cores rimmed by alkali feldspar (D'Oriano et al., 2005; Astbury et al., 2016; 2018). We are not aware of any studies reporting similar textures in pyroclastic material from the 12.9 ka Laacher See eruption (i.e., the origin of LAC_{teph}). Such textures are challenging to resolve optically in powdered samples including the tephra studied here. Further optical and microanalytical (Scanning- and Transmission Electron Microscopy) observations (e.g., Whale et al., 2017; Holden et al., 2019) will be needed to explore whether the boundary between Na- and K-rich regions in anti-rapakivi microtexture may give rise to nanoscale topography that induces effects analogous to perthitic microtexture in promoting ice nucleation."

Lastly, the Reviewer queries how such textures might be affected by milling with a zirconia ball and vial. Tephra surfaces are fractured as coarse particles are crushed down to finer particles. However, as we note on Page 7 Lines 17-21, the ability of textures such as perthite to promote ice nucleation is thought to relate to nanoscale topographical features at the boundary of Na- and K-rich phases (Whale et al., 2017; Holden et al., 2019). These nanoscale features would be preserved in milled particles ranging from tens to hundreds of nanometres to several micrometres in diameter.

Minor/Technical Comments

Page 1, Line 10: This abbreviation seems slightly confusing in the context of ice nucleation, since Vali et al. 2014 have proposed the acronym INE as "ice nucleating entity." I suggest you change INE to something like INeff"

We have changed "INE" for "ice-nucleating effectiveness" to "INA" for "ice-nucleating activity" throughout the manuscript and Supplementary Material.

Page 1, Line 15: "warmer" instead of higher?

We have substituted "warmer" into this line.

Page 1, Line 20: The word "categorically" seems excessive here.

We have removed "categorically" from this line.

Page 1, Line 28: The sentence that starts "Ice formation" is unnecessarily long. I would suggest splitting into at least two sentences. A natural break in theme occurs at "as well as."

We have split this sentence into two.

Page 1, Line 36: This sentence seems to be missing a comma and coordinating conjunction after diameter. It is the volcanic ash that is usually dominated, not the diameter that is usually dominated.

We have revised this sentence as follows:

Page 1 Lines 37-39: "By definition, volcanic ash consists of pyroclastic particles <2 mm in diameter, and is comprised of aluminosilicate glass as well as aluminosilicate and/or Fe(-Ti) oxide minerals (Heiken and Wohletz, 1992)."

Page 1, Line 36: This paragraph seems incredibly weak. Part of the problem is that many statements are weakly lumped into "and references therein." For example, there is little mention of previous work on volcanic ash. For something like dust with hundreds of studies converging on a typical behavior, this could be appropriate–however; there are few previous experiments on volcanic ash, and each of them add holistically to the story presented here.

We have added content in this paragraph relating to previous studies on volcanic ash ice nucleation:

Page 2 Lines 17-20: "In immersion freezing experiments, Soufrière Hills ash has been found to range from inactive to highly active in nucleating ice, with the discrepancy inferred to relate to differences in ash composition and sample preparation methods (Schill et al., 2015; Mangan et al., 2017; Jahn et al., 2019)."

Page 2 Lines 24-33: "There is increasing evidence that similar factors may influence ice nucleation by volcanic ash. Kulkarni et al. (2015) argued that the presence of amorphous material reduced the INA of Eyjafjallajökull ash compared to Arizona test dust, based on the notion that crystalline structures provide preferred

configurations for water molecules to bind at the particle surface (Pruppacher and Klett, 2010). Schill et al. (2015) proposed that, aside from amorphous versus crystalline content, differences in mineralogy could explain the INA of ash from Soufrière Hills, Fuego, and Taupo volcanoes. Recently, Jahn et al. (2019) suggested that feldspar and pyroxene minerals were responsible for the high INA of Soufrière Hills, Fuego, and Santiaguito ash samples. Genareau et al. (2018) conversely noted a broad trend between chemical composition and ice nucleation, with the INA of five ash samples increasing with K_2O content and decreasing with MnO content."

Page 2, Line 14: I would prefer that this sentence, if left here, explains how you "improv[ed] the understanding" instead of just simply stating that it will be done.

We have revised this sentence as follows:

Page 2 Lines 41-42/Page 3 Lines 1-2: "By finding that crystalline phases promote ash ice nucleation and that magma composition may exert an indirect effect via its influence on ash mineralogy, we contribute to an improved understanding of the potential for airborne ash from different eruptions to impact ice formation above the volcanic vent and/or once dispersed in the ambient atmosphere."

Page 2, Line 22: Since this is an atmospheric chemistry and physics journal, and not a geology journal, it would be helpful for readers of this journal to have the melting point range of each of the minerals in Table 2 compiled for them. That would greatly help them interpret the results of this study and perhaps elucidate why some samples retain some ice nucleation activity after the melt/quench cycle.

The melting points of minerals in a pure state are different from the melting points of minerals in a heterogeneous mixture such as volcanic tephra. Therefore, it would not be meaningful to report "***the melting point range of each of the minerals in Table 2***", since they would not be reflective of the actual temperature at which the tephra components melted (eutectic melting) during the process of generating the glass samples.

However, the Reviewer makes a good point in implying that the observation that "***some samples retain some ice nucleation activity after the melt/quench cycle***" might be indicative of small amounts of crystals being present in a couple of the glass samples following melting and quenching. We have inserted text to highlight this possibility in explaining the higher INA of CID_{glass} and COL_{glass} relative to the other glasses studied:

Page 8 Lines 26-28: "It is possible that CID_{glass} and COL_{glass} contain small amounts of crystals below detection by XRD that survived melting or formed during quenching, which could explain why these glasses stand out in their ability to nucleate ice."

Page 3, Line 28 and Line 37: These equations need commas after them, since you have another clause after them (starting with "where").

We have inserted commas after these equations.

Page 4, Line 10: I see why these arguments are included in this section, but they seem out of place. For example, the glassy organic particles all nucleated ice in the "deposition" mode and were certainly not immersed in water droplets at or above water saturation. I would suggest the first two sentences of this paragraph be qualified or removed.

We have removed reference here to ice nucleation by glassy organic particles.

Page 4, Line 16: As the figure looks now, there does not seem to be significant overlap with the markers and the grayed out region. Perhaps adding error bars to all curves would make that more clear? Or put error bars on the points in Figure 3?

There is considerable overlap in terms of the temperature range in which freezing of the background water and the glass sample suspensions occurs (not necessarily overlap of individual data points). We have revised the text to clarify this and, as the Reviewer suggests, we have added error bars to the $n_s(T)$ curves of the glass samples in the region of the background water in Figure 2d:

Page 5 Lines 12-15: "For the glass samples in contrast, there is significant overlap of temperatures at which their $f_{ice}(T)$ curves and those of the background water fall, spanning a range from -18 °C to -35 °C (Fig. 2b). As illustrated by the overlap of error bars in their $n_s(T)$ curves (Fig. 2d), this prevents attribution of the observed freezing to ice nucleation by glass particles and comparison of individual glass activities."

Page 6, Line 28: Or, potentially, mafic magmas with high orthopyroxene?

Please see our detailed response above to the Reviewer's second major comment, which relates to the same idea. We agree and acknowledge that pyroxene minerals, as well as feldspar minerals, could be responsible for ice nucleation by volcanic ash. However, based on experimental observations regarding the most ice-active tephra samples (COL_{teph}, TUN_{teph}, NUO_{teph}, AST_{teph}), we maintain our original speculation in the conclusion that intermediate to felsic alkaline magmas might give rise to crystalline ash that is highly ice-active (Figure 6).

Page 7, Line 20: There should be a comma between orthopyroxene and which.

We have inserted a comma here.

Page 7, Line 37: But–isn't the ash you collected from volcanic plumes where high concentrations of acidic gases likely already interacted with the ash?

The tephra samples correspond to either ash (COL_{teph}, TUN_{teph}, AST_{teph}) or pumice (LIP_{teph}, CID_{teph}, NUO_{teph}, LAC_{teph}, ETN_{teph}, KIL_{teph}), which to varying extents, likely already interacted with acidic gases and condensates while airborne and may have experienced leaching by water once deposited. However, as we note on Page 3 Lines 11-12: "All samples were crushed to fine powders in a ball mill using a zirconia ceramic ball and vial to ensure consistent treatment of the tephra and glass materials prior to ice nucleation experiments." We have inserted additional text to clarify this in the Materials and Methods:

Page 3 Lines 12-18: "This also reduced the influence of chemically-altered surfaces resulting from tephra interaction with gases and/or liquids post-eruption (e.g., Delmelle et al., 2007), by exposing fresh surfaces with chemical and mineralogical properties reflective of the source magma and any entrained lithic material. This allowed us to address the study objective of assessing specifically the role of chemical composition, crystallinity, and mineralogy on ice nucleation by volcanic ash. Aside from crushing, the samples were not processed by rinsing with water or otherwise, to avoid further alteration of these materials on short time scales (e.g., exposure to water is known to change the INA of some minerals; Harrison et al., 2016; Kumar et al., 2018)."

This is why we acknowledge on Page 9 Lines 28-41 of the Conclusion that - having studied the importance of these primary properties (chemical composition, crystallinity, mineralogy) in ice nucleation by volcanic ash - the next step is to investigate how ash surface 'aging' in the plume and the atmosphere may influence the ash INA. Such further investigations are in progress in our laboratory (e.g., Maters et al., 2019).

Figure 1 Legend: Is LEI in Figure 1 KIL everywhere else?

Yes; we have replaced "LEI" in the Figure 1 legend with "KIL" as elsewhere

Figure 2, 3, and 5. The symbols in these figures are unreasonably small, especially in print form. This makes it relatively difficult to see the different between some of the samples that have similar marker colors (e.g., green, red, light blue.)

We have amended this; enlarging the symbols in these figures to make it easier to see different sample colours, yet still small enough to distinguish individual sample curves (avoid extensive overlap of closely plotted data points).

REVIEWER #2

Specific Comments

Throughout the manuscript you refer to the vertical eruption "plume", and the laterally dispersed "cloud", as defined on line 27 of the introduction. I understand that these terms are not explicitly set by anyone, but physically, it is more correct to call the vertical part the "column" and the laterally spreading part the "plume." Calling the plume a "cloud" is not technically correct and can cause some confusion amongst atmospheric scientists.

Unfortunately, these terms are not used systematically in the literature. We have adopted terminology consistent with leading authors in the field, where the vertical component connected to the active volcanic vent is called the eruption "plume" (e.g., Herzog et al., 1998; Delmelle et al., 2007; Ayris et al., 2013; 2014; Hoshyaripour et al., 2012; 2014; Van Eaton et al., 2015). Similarly, we call the laterally dispersed component the eruption "cloud", consistent with literature referring to this more dilute feature downwind of the active volcanic vent (e.g., Rose et al., 1995; 2000; 2006; Durant et al., 2010; 2012; Van Eaton et al., 2015).

Why not refer to the ice nucleation activity (INA) instead of the ice-nucleating effectiveness (INE). INE is already used for other descriptors.

We have changed "INE" for "ice-nucleating effectiveness" to "INA" for "ice-nucleating activity" throughout the manuscript and Supplementary Material.

In the Materials and Methods section, more information on the preparation of the tephra samples is required. Were accidental lithics removed? Were the samples rinsed to remove adsorbed salts? This second question relates to the statement on page 7, line 37. Were they altered in any way following eruption? Weathering of the glass postdeposition may introduce small amounts of clay minerals into the samples that are not in high enough quantity to be detected by XRD.

In short, nothing was done to the tephra samples aside from crushing them in a ball mill. We have added text to explain the reasoning for this in the Materials and Methods:

Page 3 Lines 11-18: "All samples were crushed to fine powders in a ball mill using a zirconia ceramic ball and vial to ensure consistent treatment of the tephra and glass materials prior to ice nucleation experiments. This also reduced the influence of chemically-altered surfaces resulting from tephra interaction with gases and/or liquids post-eruption (e.g., Delmelle et al., 2007), by exposing fresh surfaces with chemical and mineralogical properties reflective of the source magma and any entrained lithic material. This allowed us to address the study objective of assessing specifically the role of chemical composition, crystallinity, and mineralogy in ice nucleation by volcanic ash. Aside from crushing, the samples were not processed by rinsing with water or otherwise, to avoid further alteration of these materials on short time scales (e.g., exposure to water is known to change the INA of some minerals; Harrison et al., 2016; Kumar et al., 2018)."

We have also added text to acknowledge the possibility of soluble salts in the tephra affecting ice nucleation in the Conclusion:

Page 9 Lines 34-39: "Moreover, it has recently been shown that even very low concentrations of soluble salts (1×10^{-4} M) can influence the INA of feldspar minerals (Whale et al., 2018; Kumar et al., 2018), and we cannot exclude the possibility that small amounts of NaCl or KCl formed by prior ash-gas/condensate interactions in our tephra samples reduced their INA. However, given the strong correlations observed between INA and composition of the crystalline tephra samples (Fig. 6), we do not think that a potential influence of soluble salts on freezing temperatures affects the general conclusions of this study."

Lastly, weathering of some of the tephra samples post-deposition could have introduced small amounts of clay minerals below detection by XRD, as the Reviewer suggests. However, clay minerals are not thought to be particularly ice-active (e.g., Atkinson et al., 2013; Augustin-Bauditz et al., 2014), and if present in such small quantities are unlikely to have driven the overall trends observed for the crystalline tephra samples, whose INAs are found to correlate well with their bulk compositional and mineralogical properties (Table 2; Figure 6).

Following milling of the tephras, was a grain size distribution analysis performed to insure the sizes of particles were consistent between samples? Although surface area was measured, the size distribution of the particles may also affect the ice nucleation (i.e., more smaller particles will increase SA compared to fewer, larger particles). Although the milling procedure should effectively homogenize the size distribution, checking this would strengthen the reliability of the results.

The Reviewer raises the idea that grain size distribution differences between samples could affect ice nucleation since more smaller particles provide greater surface area than fewer larger particles. We agree with this and hence, have normalised the ice nucleation data to the total surface area in each experiment (see Equation 2, Page 4 Lines 31-34), calculated from the sample specific surface area (in $m^2\ g^{-1}$) determined by nitrogen gas adsorption and the sample mass present in the water droplets (given a 1 wt.% suspension). Expressing the INA of samples in terms of the number of ice nucleation active sites per unit surface area ('n_s'), as done widely in literature studies of heterogeneous ice nucleation (e.g., Connolly et al., 2009; Hoose and Möhler, 2012; Zolles et al., 2015; Harrison et al., 2016; Jahn et al., 2019), implicitly accounts for differences in solid surface area provided by particles of different sizes between samples. Therefore, we do not think that there is an added value in presenting the grain size distribution of the milled samples in this study.

Although they used deposition-mode experiments, and not immersion-mode, the recent study of Kiselev et al. (2017) examined variations in ice nucleation due to defects in the crystal structure of K-feldspars. It may be worthwhile to look at this study for additional information on your interpretations. Specifically, it may be worth considering not only the presence of particular minerals, but the crystal shapes and surface attributes of these minerals, as they may also affect the likelihood of ice nucleation. This point is partly discussed on page 6, line 5, regarding the study of Whale et al. (2017), but should be explored further. I have included the Kiselev reference below. Additionally, it is mentioned on page 6, line 18, that any relevant mineral textures are difficult to resolve in powdered samples, but these samples can be easily examined in backscattered SEM mode to check for any notable mineral textures. Without knowing the size of the grains, it is difficult to say for sure.

We have added a line referring to the findings of Kiselev et al. (2017) in our discussion of the role of perthite microtexture in ice nucleation by alkali feldspar:

Page 7 Lines 17-21: "[…] the presence of perthitic intergrowth microtexture arising from phase separation (exsolution) into Na- and K-rich regions. Strain at the boundary of these regions gives rise to nanoscale topographic features that are suggested to be important in generating sites for ice nucleation (Whale et al., 2017; Holden et al., 2019). It may be that these features stabilise patches of the high-energy (100) crystallographic plane exposed by surface defects, which Kiselev et al. (2017) showed to be favourable sites for ice nucleation on alkali feldspar."

Unfortunately, in heterogeneous materials such as the studied tephra, it is challenging to isolate individual crystal faces of alkali feldspar to check for such textures. Kiselev et al. (2017), Whale et al. (2017), and Holden

et al. (2019) worked with macroscopic alkali feldspar substrates prepared/oriented to expose particular crystallographic planes (e.g., in the form of thin sections) for examination by high-resolution microscopy. The nature of our powdered samples does not readily allow for this mode of investigation.

Technical Corrections

Line 19 of the abstract: delete the word "partly"

We have deleted "partly" from this line.

The sentence beginning on page 2, line 35 just sounds awkward and should be rephrased.

We have rephrased this sentence:

Page 2 Lines 2-4: "As magma ascends to the surface, the aluminosilicate melt typically carries a cargo of mineral species in the form of crystals suspended within and originating from the melt and/or from the surrounding country rock."

The third and fourth paragraphs in section 2.1 are not materials or methods and should be placed somewhere else, perhaps the introduction?

We have moved the content of these paragraphs to the Introduction.

Page 7, line 21, tephra should be plural.

We have corrected this.

Can you discuss further the characteristics of pyroxene minerals that might influence their ice nucleation abilities?

It is difficult to discuss "***the characteristics of pyroxene minerals that might influence their ice nucleation abilities***" when this information is simply not in the literature. Even the characteristics of (the more comprehensively studied) feldspar minerals that influence their ice nucleation abilities are far from fully understood. We have inserted a few lines to explain that pyroxene is:

Page 7 Lines 40-43/Page 8 Lines 1-2: "[…] an aluminosilicate mineral group of the general formula XYZ_2O_6, where X and Y are often Mg^{2+}, Fe^{2+} or Ca^{2+} and Z is Si^{4+} or sometimes Al^{3+} (Morimoto et al., 1988). A solid solution exists between the $Mg_2Si_2O_6$ and $Fe_2Si_2O_6$ end-members with small amounts of Ca^{2+} substitution possible (orthopyroxenes), whereas solid immiscibility occurs between other compositions particularly with higher Ca^{2+} content (clinopyroxenes)."

However, very little research has been done on the ability of pyroxene minerals to nucleate ice, likely because they typically do not occur as a component in desert dust. A very recent study that measured ice nucleation by a clinopyroxene specimen (diopside-augite) concluded that the cause of its INA "is unknown but could be due to any of the variety of mineralogical properties […] such as crystal lattice match, surface functional group distribution, and topographical features" (Jahn et al., 2019). This warrants investigation and is outside the scope of the current study. We acknowledge (Page 8 Lines 12-13) that "additional research is needed to quantify the INA of a range of pyroxene minerals," to which we have added "and probe the nature of their ice-nucleating properties", and this is in progress in our laboratory (Maters et al., in prep.). We therefore prefer to reserve further discussion of this topic for a future study.

I don't quite understand the point of plotting both the tephras and glasses in Figure 1a, since they directly overlap in most cases.

Figure 1b (formerly 1a) illustrates that the nine tephra-glass pairs span a range of compositions in terms of Total Alkali versus Silica classification. Showing that the individual tephra and glass samples in each pair "***directly overlap in most cases***" importantly demonstrates that the two materials are nearly identical in overall chemical composition (i.e., it does not change when the tephra is remelted/quenched to produce the glass).

When reporting the INE (Tns ~ 1 cm -2) throughout the text, why is the 1 so small…is it subscripted?

Yes; "$n_s \approx 1\ cm^{-2}$" refers to an 'ice-active surface site density approximately equal to one per square centimetre' and, therefore, this entire expression is subscripted to accurately designate that we are referring to the temperature "T" at which this occurs.

Please state in the caption of Table S1 that these are XRF measurements.

We have specified in the Table S1 caption that the bulk chemical composition was "determined by X-ray fluorescence".

Please state in the caption of Table S2 that these are XRF measurements.

We have specified in the Table S2 caption that the feldspar chemical composition was "determined by electron microprobe analysis" (not by X-ray fluorescence).

Is the "Text S1" mislabeled? I think the supplementary tables are not currently labeled correctly. Should they be: Table S1 (XRF measurements of bulk samples); Table S2 (Electron microprobe measurements of tephra glasses; Table S3 (Electron microprobe measurements of feldspars).

The Supplementary Material content is labelled correctly. Table S1 presents X-ray fluorescence measurements of bulk samples (tephras and glasses), Text S1 provides details of the electron microprobe analysis technique, and Table S2 presents electron microprobe measurements of feldspars in the tephras. There are only two tables in the Supplementary Material.

Figures 4, 6, S1, and S2 need to include error bars or a statement of the errors in the captions.

We have inserted error bars in Figures 4, 6, S1, and S2. They are very small and typically cannot be seen to extend beyond the data symbols.

REFERENCES

Astbury, R. L., Petrelli, M., Arienzo, I., D'Antonio, M., Morgavi, D., and Perugini, D.: Using trace element mapping to identify discrete magma mixing events from the Astroni 6 eruption, in: American Geophysical Union Fall Meeting 2016, San Francisco, United States of America, 12-16 December 2016, 2016AGUFM.V33E3176A, 2016.

Astbury, R. L., Petrelli, M., Ubide, T., Stock, M. J., Arienzo, I., D'Antonio, M., and Perugini, D.: Tracking plumbing system dynamics at the Campi Flegrei caldera, Italy: High-resolution trace element mapping of the Astroni crystal cargo, Lithos, 318-319, 464-477, https://doi.org/10.1016/j.lithos.2018.08.033, 2018.

Atkinson, J. D., Murray, B. J., Woodhouse, M. T., Whale, T. F., Baustian, K. J., Carslaw, K. S., Dobbie, S., O'Sullivan, D., and Malkin, T. L.: The importance of feldspar for ice nucleation by mineral dust in mixed-phase clouds, Nature, 498, 355-358, doi:10.1038/nature12278, 2013.

Augustin-Bauditz, S., Wex, H., Kanter, S., Ebert, M., Niedermeier, D., Stolz, F., Prager, A., and Stratmann, F.: The immersion mode ice nucleation behavior of mineral dusts: A comparison of different pure and surface modified dusts, Geophys. Res. Lett., 41, 7375–7382, doi:10.1002/2014GL061317, 2014.

Ayris, P. M., Lee, A. F., Wilson, K., Kueppers, U., Dingwell, D. B., and Delmelle, P.: SO_2 sequestration in large volcanic eruptions: high-temperature scavenging by tephra, Geochim. Cosmochim. Ac., 110, 58-69, https://doi.org/10.1016/j.gca.2013.02.018, 2013.

Ayris, P. M., Delmelle, P., Cimarelli, C., Maters, E. C., Suzuki, Y. J., and Dingwell, D. B.: HCl uptake by volcanic ash in the high temperature eruption plume: Mechanistic insights, Geochim. Cosmochim. Ac., 144, 188-201, https://doi.org/10.1016/j.gca.2014.08.028, 2014.

Connolly, P. J., Möhler, O., Field, P. R., Saathoff, H., Burgess, R., Choularton, T., and Gallagher, M.: Studies of heterogeneous freezing by three different desert dust samples, Atmos. Chem. Phys., 9, 2805–2824, doi:10.5194/acp-9-2805-2009, 2009.D'Oriano, C., Poggianti, E., Bertagnini, A., Cioni, R., Landi, P., Polacci, M., and Rosi, M.: Changes in eruptive style during the A.D. 1538 Monte Nuovo eruption (Phlegrean Fields, Italy): the role of syn-eruptive crystallization, B. Volcanol., 67, 601-621, doi:10.1007/s00445-004-0397-z, 2005.

Delmelle, P., Lambert, M., Dufrêne, Y., Gerin, P., and Óskarsson, N.: Gas/aerosol-ash interaction in volcanic plumes: New insights from surface analysis of fine ash particles, Earth Planet Sc. Lett., 259, 159-170, https://doi.org/10.1016/j.epsl.2007.04.052, 2007.

D'Oriano, C., Poggianti, E., Bertagnini, A., Cioni, R., Landi, P., Polacci, M., and Rosi, M.: Changes in eruptive style during the A.D. 1538 Monte Nuovo eruption (Phlegrean Fields, Italy): the role of syn-eruptive crystallization, B. Volcanol., 67, 601-621, doi:10.1007/s00445-004-0397-z, 2005.

Durant, A. J., Bonadonna, C., and Horwell, C. J.: Atmospheric and environmental impacts of volcanic particulates, Elements, 6, 235-240, doi:10.2113/gselements.6.4.235, 2010.

Durant, A. J., Villarosa, G., Rose, W. I., Delmelle, P., Prata, A. J., and Viramonte, J. G.: Long-range volcanic ash transport and fallout during the 2008 eruption of Chaitén volcano, Chile, Phys. Chem. Earth, 45-46, 50-64, doi:10.1016/j.pce.2011.09.004, 2012.

Genareau, K., Cloer, S. M., Primm, K., Tolbert, M. A., and Woods, T. W.: Compositional and mineralogical effects on ice nucleation activity of volcanic ash, Atmosphere, 9, 238, https://doi.org/10.3390/atmos9070238, 2018.

Harrison, A. D., Lever, K., Sanchez-Marroquin, A., Holden, M. A., Whale, T. F., Tarn, M. D., McQuaid, J. B., and Murray, B. J.: The ice-nucleating ability of quartz immersed in water and its atmospheric importance compared to K-feldspar. In preparation for Atmos. Chem. Phys.

Harrison, A. D., Whale, T. F., Carpenter, M. A., Holden, M. A., Neve, L., O'Sullivan, D., Vergara Temprado, J., and Murray B. J.: Not all feldspars are equal: a survey of ice nucleating properties across the feldspar group of minerals, Atmos. Chem. Phys., 16, 10927-10940, https://doi.org/10.5194/acp-16-10927-2016, 2016.

Heiken, G., and Wohletz, K. (Eds.): Volcanic Ash, University of California Press, London, United Kingdom, 1992.

Herzog, M., Graf, H. F., Textor, C., and Oberhuber, J. M.: The effect of phase changes of water on the development of volcanic plumes. J. Volcanol. Geoth. Res., 87, 55-74, https://doi.org/10.1016/S0377-0273(98)00100-0, 1998.

Holden, M. A., Whale, T. F., Tarn, M. D., O'Sullivan, D., Walshaw, R. D., Murray, B. J., Meldrum, F. C., and Christenson, H. K.: High-speed imaging of ice nucleation in water proves the existence of active sites, Sci. Adv., 5, eaav4316, doi: 10.1126/sciadv.aav4316, 2019.

Hoose, C., and Möhler, O.: Heterogeneous ice nucleation on atmospheric aerosols: a review of results from laboratory experiments, Atmos. Chem. Phys., 12, 9817–9854, doi:10.5194/acp-12-9817-2012, 2012.

Hoshyaripour, G., Hort, M., and Langmann, B.: How does the hot core of a volcanic plume control the sulfur speciation in volcanic emission? Geochem Geophy Geosy, 13, Q07004, https://doi.org/10.1029/2011GC004020, 2012.

Hoshyaripour, G., Hort, M., Langmann, B., and Delmelle, P.: Volcanic controls on ash iron solubility: New insights from high-temperature gas-ash interaction modelling, J. Volcanol. Geoth. Res., 286, 67-77, https://doi.org/10.1016/j.jvolgeores.2014.09.005, 2014.

Jahn, L., Fahy, W., Williams, D. B., and Sullivan, R. C.: The role of feldspar and pyroxene minerals in the ice nucleating ability of three volcanic ashes, ACS Earth Space Chem., XX, XX-XX, doi:10.1021/acsearthspacechem.9b00004, 2019.

Kiselev, A., Bachmann, F., Pedevilla, P., Cox, S. J., Michaelides, A., Gerthsen, D., and Leisner, T.: Active sites in heterogeneous ice nucleation – the example of K-rich feldspars, Science, 355, 367-371, doi:10.1126/science.aai8034, 2017.

Kulkarni, G., Nandasiri, M., Zelenyuk, A., Beranek, J., Madaan, N., Devaraj, A., Shutthanandan, V., Thevuthasan, S., and Varga, T.: Effects of crystallographic properties on the ice nucleation properties of volcanic ash particles, Geophys. Res. Lett., 42, 3048-3055, https://doi.org/10.1002/2015GL063270, 2015.

Kumar, A., Marcolli, C., and Peter, T.: Ice nucleation activity of silicates and aluminosilicates in pure water and aqueous solutions. Part 3 – Aluminosilicates, Atmos. Chem. Phys. Discuss., https://doi.org/10.5194/acp-2018-1021, 2018.

Mangan, T. P., Atkinson, J. D., Neuberg, J. W., O'Sullivan, D., Wilson, T. W., Whale, T. F., Neve, L., Umo, N. S., Malkin, T. L., and Murray, B. J.: Heterogeneous ice nucleation by Soufriere Hills volcanic ash immersed in water droplets, PloS ONE, 12, e0169720, https://doi.org/10.1371/journal.pone.0169720, 2017.

Maters, E. C., Casas, A. S., Dingwell, D. B., Corrado, C., and Murray, B. J.: Alteration of the ice-nucleating effectiveness of volcanic ash by high temperature ash-gas interactions, presented at VMSG 2019 Annual Meeting, St. Andrews, Scotland, 8-10 January 2019.

Maters, E. C., Harrison, A. D., Whale, T. F., and Murray, B. J.: The ice-nucleating activity of various pyroxene minerals in the immersion mode, in preparation for J. Geophys. Res. Atmos.

Morimoto, N., Fabries, J., Ferguson, A. K., Ginzburg, I. V., Ross, M., Seifert, F. A., and Zussman, J.: Nomenclature of pyroxenes, Miner. Petrol., 39, 55-76, https://doi.org/10.1007/BF01226262, 1988.

Parsons, I., Fitz Gerald, J. D., Lee, M. R.: Routine characterization and interpretation of complex alkali feldspar intergrowths, Am. Mineral., 100, 1277-1303, https://doi.org/10.2138/am-2015-5094, 2015.

Peckhaus, A., Kiselev, A., Hiron, T., Ebert, M., and Leisner, T.: A comparative study of K-rich and Na/Ca-rich feldspar ice-nucleating particles in a nanoliter droplet freezing assay, Atmos. Chem. Phys., 16, 11477-11496, doi:10.5194/acp-16-11477-2016, 2016.

Rose, W. I., Delene, D. J., Schneider, D. J., Bluth, G. J. S., Krueger, A. J., Sprod, I., McKee, C., Davies, H. L., and Ernst, G. G. J.: Ice in the 1994 Rabaul eruption cloud: implications for volcano hazard and atmospheric effects, Nature, 375, 477-479, doi:10.1038/375477a0, 1995.

Rose, W. I., Bluth, G. J. S., and Ernst, G. G. J.: Integrating retrievals of volcanic cloud characteristics from satellite remote sensors: a summary, Phil. Trans. R. Soc. Lond. A, 358, 1585-1606, https://doi.org/10.1098/rsta.2000.0605, 2000.

Rose, W. I., Millar, G. A., Mather, T. A., Hunton, D. E., Anderson, B., Oppenheimer, C., Thornton, B. F., Gerlach, T. M., Viggiano, A. A., Kondo, Y., Miller, T. M., and Ballenthin, J. O.: Atmospheric chemistry of a 33–34 hour old volcanic cloud from Hekla Volcano (Iceland): Insights from direct sampling and the application of chemical box modeling, J. Geophys. Res., 111, D20206, doi:10.1029/2005JD006872, 2006.

Schill, G. P., Genareau, K., and Tolbert, M. A.: Deposition and immersion-mode nucleation of ice by three distinct samples of volcanic ash, Atmos. Chem. Phys., 15, 7523-7536, https://doi.org/10.5194/acp-15-7523-2015, 2015.

Van Eaton, A. R., Mastin, L. G., Herzog, M., Schwaiger, H. F., Schneider, D. J., Wallace, K. L., and Clarke, A. B.: Hail formation triggers rapid ash aggregation in volcanic plumes, Nat. Commun., 6, 7860, https://doi.org/10.1038/ncomms8860, 2015.

Welti, A., Lohmann, U., and Kanji, Z. A.: Ice nucleation properties of K-feldspar polymorphs and plagioclase feldspars, Atmos. Chem. Phys. Discuss., https://doi.org/10.5194/acp-2018-1271, 2019.

Whale, T. F., Holden, M. A., Kulak, A. N., Kim, Y.-Y., Meldrum, F. C., Christenson, H. K., and Murray, B. J.: The role of phase separation and related topography in the exceptional ice-nucleating ability of alkali feldspars, Phys. Chem. Chem. Phys., 19, 31186-31193, doi:10.1039/c7cp04898j2, 2017.

Whale, T. F., Holden, M. A., Wilson, T. W., O'Sullivan, D., and Murray, B. J.: The enhancement and suppression of immersion mode heterogeneous ice-nucleation by solutes, Chem. Sci., 9, 4142-4151, doi:10.1039/c7sc05421a, 2018.

Zolles, T., Burkart, J., Häusler, T., Pummer, B., Hitzenberger, R., and Grothe, H.: Identification of ice nucleation active sites on feldspar dust particles, J. Phys. Chem. A, 119, 2692-2700, doi:10.1021/jp509839x, 2015.

The importance of crystalline phases in ice nucleation by volcanic ash

Elena C. Maters[1], Donald B. Dingwell[2], Corrado Cimarelli[2], Dirk Müller[2], Thomas F. Whale[1,3], Benjamin J. Murray[1]

[1]School of Earth and Environment, University of Leeds, Leeds LS2 9JT, United Kingdom
[2]Department of Earth and Environmental Sciences, Ludwig-Maximilians University, 80333 Munich, Germany
[3]School of Chemistry, University of Leeds, Leeds LS2 9JT, United Kingdom

Correspondence to: Elena C. Maters (e.c.maters@leeds.ac.uk)

Abstract. Volcanic ash is known to nucleate ice when immersed in supercooled water droplets. This process may impact the properties and dynamics of the eruption plume and cloud, as well as those of meteorological clouds once the ash is dispersed in the atmosphere. However, knowledge of what controls the ice-nucleating ~~effectiveness~~ activity (IN~~E~~A) of ash remains limited, although it has been suggested that crystalline components in ash may play an important role. Here we adopted a novel approach using nine pairs of tephra and their remelted and quenched glass equivalents to investigate the influence of chemical composition, crystallinity and mineralogy on ash IN~~E~~A in the immersion mode. For all nine pairs studied, the crystal-bearing tephra nucleated ice at ~~higher~~warmer temperatures than the corresponding crystal-free glass, ~~demonstrat~~indicating that crystalline phases are key to ash IN~~E~~A. Similar to findings for desert dust from arid and semi-arid regions, the presence of feldspar minerals characterises the four most ice-active tephra samples, although a high IN~~E~~A is observed even in the absence of alkali feldspar in samples bearing plagioclase feldspar and orthopyroxene. There is evidence of a potential indirect relationship between chemical composition and ash IN~~E~~A, whereby a magma of felsic to intermediate composition may generate ash containing ice-active feldspar or pyroxene minerals. This complex interplay between chemical composition, crystallinity, and mineralogy could help ~~partly~~ to explain the variability in volcanic ash IN~~E~~A reported in the literature. Overall, by ~~categorically~~ demonstrating the importance of crystalline phases in the IN~~E~~A of ~~volcanic~~ ash, our study contributes insights essential for better appraising the role of airborne ash in ice formation. Among these is the inference that glass-dominated ash emitted by the largest explosive volcanic eruptions m~~ay~~ight be less effective at impacting ice-nucleating particle populations than crystalline ash generated by smaller, more frequent eruptions.

1 Introduction

Volcanic ash produced by explosive eruptions can act as ice-nucleating particles (INPs), promoting heterogeneous freezing of supercooled water in the vertical eruption plume, the laterally dispersed eruption cloud, and the wider atmosphere (Isono et al., 1959a; 1959b; Hobbs et al., 1971; Rose et al., 2003). Ice formation in these contexts is poorly understood yet may exert a profound influence on eruption plume/cloud dynamics and electrification (e.g., Herzog et al., 1998; Cimarelli et al., 2016), sequestration of gaseous species (e.g., Textor et al., 2003; Guo et al., 2004a), and ash aggregation and sedimentation (e.g., Guo et al., 2004b; Van Eaton et al., 2015)~~,~~. Ice formation on airborne ash can also affect~~as well as~~ atmospheric cloud properties and lifetime (e.g., Komabayasi, 1957; Seifert et al., 2011), and thereby the hydrological cycle and climate (e.g., Isono and Komabayasi, 1954). Ongoing volcanic activity generates a recurrent flux of ash particles into the atmosphere (176-256 Tg a^{-1}; Durant et al., 2010), whereas sporadic large eruptions can result in ash loadings greatly exceeding annual averages over very short (hour to day) time scales and transiently dominating INP populations (e.g., Isono et al., 1959a; 1959b; Hobbs et al., 1971).

By definition, volcanic ash consists of pyroclastic particles <2 mm in diameter, ~~usually dominated by~~ and is comprised of aluminosilicate glass ~~derived from the melt and/or~~ as well as aluminosilicate and/or Fe(-Ti) oxide minerals ~~in the form of crystals suspended within the original melt~~ (Heiken and Wohletz, 1992). The chemical composition of ~~volcanic~~ ash

predominantly reflects the state of the source magma at the point of eruption but can also be influenced by lithic material (pre-existing country rock) entrained during the ~~explosive~~ eruption (Heiken and Wohletz, 1992). As magma ascends to the surface ~~prior to a volcanic eruption~~, the aluminosilicate melt typically carries a cargo of mineral species in the form of crystals suspended within and ~~predominantly~~ originating from the melt and/or from the surrounding country rock. Accordingly, ~~U~~upon magma fragmentation, the ash generated comprises a ~~corresponding~~ mixture of glass and crystal components (Heiken and Wohletz, 1992). The crystallinity refers to the relative abundance of crystals in ash (i.e., crystal mass/total mass) and typically ranges from 0 to 65 wt.%, depending on factors such as the prior state of the magma (e.g., chemical composition, temperature) and even the dynamics of the conduit (e.g., ~~such as the ascent rate of the~~ magma ascent rate; ~~(~~Heiken and Wohletz, 1992; Wright et al., 2012). The incorporation of lithic material from the conduit or vent and/or the interaction with ground or surface water can also influence the crystallinity of the bulk erupted ash. The mineralogy refers to the identities and abundances of crystalline phases in ash. Among the factors that influence crystallisation from the melt~~,~~; the chemical composition of the magma is a key determinant of the mineral phases that can form (Heiken and Wohletz, 1992). Common mafic minerals in basaltic ash include pyroxene, olivine, amphibole, and (Ca-rich) plagioclase feldspar, whereas ~~those~~felsic minerals in rhyolitic ash include quartz, mica, amphibole, (Na-rich) plagioclase feldspar, and (K-rich) alkali feldspar (Fig. 1~~b~~a; Rogers, 2015).

Field and laboratory measurements present conflicting evidence as to the ice-nucleating ~~effectiveness~~activity (IN~~E~~A) of ash (e.g., Isono et al., 1959a; Hobbs et al., 1971; Schnell and Delany, 1976; Schnell et al., 1982), even for samples from the same volcano, and it is far from clear what drives this variation (Durant et al., 2008~~, and references therein; Mangan et al., 2017~~). In immersion freezing experiments, Soufrière Hills ash has been found to range from inactive to highly active in nucleating ice, with the discrepancy inferred to relate to differences in ash composition and sample preparation methods (Schill et al., 2015; Mangan et al., 2017; Jahn et al., 2019). Studies on desert dust from arid and semi-arid regions (1000-3000 Tg a^{-1} emitted; Penner et al., 2001) - considered one of the most important INP types globally (Hoose et al., 2010; Vergara-Temprado et al., 2017) - suggest that chemical composition, crystallinity and mineralogy can influence the abundance of ice-active surface sites on the solid particles (Murray et al., 2012, and references therein). Specifically, the presence of K-rich feldspar is thought to dominate the IN~~E~~A of dust (Atkinson et al., 2013; Yakobi-Hancock et al., 2013; Kaufmann et al., 2016). There is increasing evidence that s~~S~~imilar factors may~~ight~~ influence ice nucleation by volcanic ash ~~(Kulkarni et al., 2015; Schill et al., 2015; Genareau et al., 2018)~~. Kulkarni et al. (2015) argued that the presence of amorphous material reduced the INA of Eyjafjallajökull ash compared to Arizona test dust, based on the notion that crystalline structures provide preferred configurations for water molecules to bind at the particle surface (Pruppacher and Klett, 2010). Schill et al. (2015) proposed that, aside from amorphous versus crystalline content, differences in mineralogy could explain the INA of ash from Soufrière Hills, Fuego, and Taupo volcanoes. Recently, Jahn et al. (2019) suggested that feldspar and pyroxene minerals were responsible for the high INA of Soufrière Hills, Fuego, and Santiaguito ash samples. Genareau et al. (2018) conversely noted a broad trend between chemical composition and ice nucleation, with the INA of five ash samples increasing with K_2O content and decreasing with MnO content. To date however, the roles and potential interplay of differing physicochemical attributes in determining a solid particle's IN~~E~~A remain poorly understood, having rarely been systematically investigated for any ice-nucleating material let alone volcanic ash.

Here we examine the influence of three properties dictated primarily by the state of the erupted source magma - chemical composition, crystallinity, and mineralogy - on the IN~~E~~A of volcanic ash in the immersion mode, which is likely relevant to ash particles in the water-rich eruption plume/cloud and in mixed-phase atmospheric clouds (Textor et al., 2006; McNutt and Williams, 2010; Pruppacher and Klett, 2010; Murray et al., 2012). To assist in disentangling the individual effects of these properties on ice nucleation, we have adopted a novel approach of sample selection by using a wide range of natural tephra *and* their remelted and quenched glass equivalents. ~~In this manner,~~ By finding that crystalline phases promote ash ice nucleation and that magma composition may exert an indirect effect via its influence on ash mineralogy, we ~~aim to~~ contribute

to an improv~~inged~~ understanding of the potential for airborne ash from different eruptions to impact ice formation above the volcanic vent and/or once dispersed in the ambient atmosphere.

2 Materials and methods

2.1 Volcanic tephra and glass samples

Eighteen tephra and (remelted and quenched) glass powders spanning a range of compositions associated with volcanic activity were studied (Table 1). The powders are represented by an abbreviated sample code with the subscripts 'teph' or 'glass' used to designate tephra or glass material, respectively. The tephra samples correspond to ash or pumice originating from different eruptions. The glass samples were synthesised by melting a portion of the tephra at 1400 to 1600 °C, homogenising the melts by stirring for 12 to 72 h, and quenching the melts at room temperature to form glasses. This technique for generating volcanic glass has been used previously in studies of volcanic ash reactivity (e.g., Ayris et al., 2013; 2014; Maters et al., 2016; 2017). All samples were crushed to fine powders in a ball mill using a zirconia ceramic ball and vial~~,~~ to ensure consistent treatment of the tephra and glass materials prior to ice nucleation experiments. This also reduced the influence of chemically-altered surfaces resulting from tephra interaction with gases and/or liquids post-eruption (e.g., Delmelle et al., 2007), by exposing fresh surfaces with chemical and mineralogical properties reflective of the source magma and any entrained lithic material. This allowed us to address the study objective of assessing specifically the role of chemical composition, crystallinity, and mineralogy in ice nucleation by volcanic ash. Aside from crushing, the samples were not processed by rinsing with water or otherwise, to avoid further alteration of these materials on short time scales (e.g., exposure to water is known to change the INA of some minerals; Harrison et al., 2016; Kumar et al., 2018). The specific surface area (SSA_{BET}; Table 1) of the samples after overnight degassing was obtained from a ten-point N_2 adsorption isotherm at -196 °C based on the Brunauer, Emmet and Teller model (Brunauer et al., 1938) using a Micromeritics TriStar 3000 instrument.

~~The chemical composition of volcanic ash predominantly reflects the state of the source magma at the point of eruption but can also be influenced by lithic material (pre-existing country rock) entrained during the explosive eruption (Heiken and Wohletz, 1992).~~ The chemical composition of the tephra and glass samples ~~studied here~~ (Table S1) was measured ~~by Nora Groschopf (Institute of Geosciences, Johannes Gutenberg University Mainz, Germany)~~ by X-ray fluorescence at 3.2 kW ionisation energy using a Philips Analytical MagiX PRO spectrometer. The conventional classification of these materials according to total alkali ($Na_2O + K_2O$) versus silica (SiO_2) content is shown on a Total Alkali versus Silica diagram in Fig. 1b~~a~~ (Le Maitre et al., 2002).

~~As magma ascends to the surface prior to a volcanic eruption, the aluminosilicate melt typically carries a cargo of mineral species in the form of crystals predominantly originating from the melt. Upon magma fragmentation, the ash generated comprises a corresponding mixture of glass and crystal components (Heiken and Wohletz, 1992). The crystallinity refers to the relative abundance of crystals in ash (i.e., crystal mass/total mass) and typically ranges from 0 to 65 wt.%, depending on factors such as the prior state of the magma (e.g., chemical composition, temperature) and even the dynamics of the conduit such as the ascent rate of the magma (Heiken and Wohletz, 1992; Wright et al., 2012). The incorporation of lithic material from the conduit or vent and/or the interaction with ground or surface water can also influence the crystallinity of the bulk erupted ash.~~

~~The mineralogy refers to the identities and abundances of crystalline phases in ash. Among the factors that influence crystallisation from the melt, the chemical composition of the magma is a key determinant of the mineral phases that can form (Heiken and Wohletz, 1992). Common minerals in basaltic ash include pyroxene, olivine, amphibole, and (Ca-rich) plagioclase feldspar, whereas those in rhyolitic ash include quartz, mica, amphibole, (Na-rich) plagioclase feldspar, and (K-rich) alkali~~

~~feldspar (Fig. 1b; Rogers, 2015). Note that in this study, we use the terms 'plagioclase' and 'alkali' to refer specifically to Na-/Ca-rich and K-rich feldspars, respectively.~~

The proportions of various crystalline phases in the tephra ~~studied here~~samples (Table 2) were determined by X-ray diffraction (XRD) with a $Cu_{K\alpha1}$ X-ray beam using a GE diffractometer (XRD 3003 TT) and the Profex software program for Rietveld refinement (Döbelin and Kleeberg, 2015). Briefly, this involved crushing the tephra and spiking it with a known mass (~17 wt.%) of pure Si powder, as crystalline internal standard, to quantify the crystallinity and mineralogy of the samples. Note that in this study, we use the terms '~~plagioclase~~alkali' and '~~alkali~~plagioclase' to refer specifically to ~~Na-/Ca~~K-rich and ~~K~~Na-/Ca-rich feldspars, respectively. While the LIP_{teph} and CID_{teph} crystallinities cannot be quantified below the ~2 wt.% ~~detection~~ limit of the technique, this does not rule out the possibility of smaller amounts of crystals and/or nanoscale crystallites being present in these samples. These minor components are listed along with the quantitative mineralogy of the tephra samples in Table 2. The glasses were also analysed by XRD to confirm their amorphous nature (i.e., the absence of crystalline minerals within the ~2 wt.% ~~detection~~ quantification limit).

2.2 Immersion mode ice nucleation experiments

The IN~~E~~A of the tephra and glass samples was assessed using a microlitre Nucleation by Immersed Particles Instrument (µL-NIPI). This instrument has been described in detail elsewhere (Whale et al., 2015) and has been used previously to study heterogeneous ice nucleation by mineral and ash material (e.g., Atkinson et al., 2013; Harrison et al., 2016; Mangan et al., 2017; Whale et al., 2017). Briefly, a 1 wt.% sample suspension in Milli-Q water (18.2 MΩ·cm) was shaken for a few minutes by a vortex mixer, and then pipetted in an array of 30 to 40 1 µL droplets onto a hydrophobic silanised glass cover slip placed on a temperature-controlled stage (Grant-Asymptote EF600 Stirling Cryocooler). The stage was cooled from room temperature at a rate of -5 °C min^{-1} down to 0 °C, and subsequently at a rate of -1 °C min^{-1} until all droplets were frozen. A dry nitrogen flow (~0.2 L min^{-1}) over the droplets prevented condensation and frost accumulation on the cover slip and hence served to avoid frozen droplets affecting neighbouring liquid droplets. A digital camera was used to observe the droplets throughout the experiment and determine the fraction of droplets frozen as a function of temperature $f_{ice}(T)$ according to:

$$f_{ice}(T) = n_{ice}(T)/n, \quad (1)$$

where $n_{ice}(T)$ is the cumulative number of droplets frozen at temperature (T) and n is the total number of droplets in the experiment. At least three replicate experiments were conducted for each sample. In addition, ice nucleation of the background water at higher temperatures than those predicted by classical nucleation theory (Murray et al., 2010~~a~~; Koop and Murray, 2016), due to impurities in the water and/or effects of the cover slip (Polen et al., 2018), was assessed by acquiring baseline droplet freezing measurements of water containing no added particles.

To facilitate comparison of different materials including across literature studies, their ability to nucleate ice is often expressed in terms of the ice nucleation active site density $n_s(T)$, which represents the number of active sites per unit surface area of a solid sample on cooling from 0 °C down to temperature (T) (Connolly et al., 2009):

$$\frac{n_{ice}(T)}{n} = 1 - \exp(-n_s(T)A), \quad (2)$$

where A is the total surface area of the solid sample per droplet. Although the fundamental nature of ice-active sites remains unclear, and may vary across different materials, $n_s(T)$ allows us to empirically define the IN~~E~~A of a range of solid substrates (Vali, 2014). The uncertainty in $n_s(T)$ was calculated using simulations of possible active site distributions propagated with the uncertainty in surface area of nucleant per droplet, as outlined in Harrison et al., (2016). The uncertainty in temperature for the µL-NIPI is estimated to be ±0.4 °C (Whale et al., 2015).

3 Results

The $f_{ice}(T)$ and $n_s(T)$ values for the eighteen samples studied are shown in Fig. 2. For the sake of clarity, droplet freezing events across replicate experiments have been combined here to generate a single dataset for each sample. The samples display wide variation in freezing temperatures with generally higher values associated with the tephra (-3 to -25 °C; Fig. 2a, c) than with the glass (-12 to -30 °C; Fig. 2b, d).

For the tephra samples, the $f_{ice}(T)$ curves are separate from those of the background water (Fig. 2a). This gives confidence to attribution of the observed freezing to ice nucleation by tephra particles. In terms of ice nucleation active site densities (Fig. 2c), taking the temperature at which $n_s \approx 1$ cm^{-2} as a simple single-number proxy for IN~~E~~A ($T_{n_s \approx 1\ cm^{-2}}$), the most active tephra are the trachyphonolite samples NUO_{teph} and AST_{teph} with $T_{n_s \approx 1\ cm^{-2}}$ values of -5.0 °C and -6.4 °C, respectively, followed by the andesite samples COL_{teph} and TUN_{teph} with $T_{n_s \approx 1\ cm^{-2}}$ values of -8.1 °C and -10.5 °C, respectively. The least active tephra are the basalt and phonolite samples KIL_{teph} and LAC_{teph} with $T_{n_s \approx 1\ cm^{-2}}$ values of -17.5 °C and -17.9 °C, respectively.

For the glass samples in contrast, there is significant overlap of temperatures at which their $f_{ice}(T)$ curves and those of the background water fall, spanning ~~temperatures from~~ a range from -18 °C to -35 °C (Fig. 2b). As illustrated by the overlap of error bars in their $n_s(T)$ curves (Fig. 2d), ~~T~~this prevents attribution of the observed freezing to ice nucleation by glass particles and comparison of individual glass activities. It also likely explains the poorer reproducibility seen in replicate experiments of the glass material relative to the tephra material (Fig. 3). Hence, in most cases the reported $n_s(T)$ values should be regarded as upper limits. However, the trachyte and andesite samples CID_{glass} and COL_{glass} stand out with only partial overlap of $f_{ice}(T)$ curves and the freezing temperature range of the background water (Fig. 2b), and thus are identified as being the most active glasses in terms of ice nucleation active site densities (Fig. 2d), with $T_{n_s \approx 1\ cm^{-2}}$ values of -16.8 °C and -17.0 °C, respectively.

Consideration of the compositionally analogous tephra-glass pairs clearly illustrates the observation of tephra nucleating ice more effectively than the equivalent remelted and quenched glass (Fig. 3). The $n_s(T)$ curves of each tephra sample fall at higher temperatures compared to those of its counterpart glass sample, albeit displaying varying temperature differences between them.

4 Discussion

The eighteen samples were chosen to encompass a variety of chemical compositions, crystallinities and mineralogies encountered in volcanic ash, with the aim of investigating the influence of these physicochemical properties on ash IN~~E~~A. The results of our ice nucleation experiments are examined in relation to each of these properties below.

4.1 Crystallinity

As noted above, our sample pairs of crystal-bearing tephra and crystal-free glass of nearly identical chemical composition (Table S1) constitute a ~~novel~~ unique approach to studying controls on volcanic ash ice nucleation. These pairs were chosen to disentangle variation in crystallinity from that in composition, which together might complicate interpretation of IN~~E~~A trends in natural ash collections. For all ~~nine~~ pairs studied, the tephra nucleates ice at higher temperatures than the corresponding glass (Fig. 3), overall implying a positive effect of crystals on IN~~E~~A. Even the dominantly glassy LIP_{teph} and CID_{teph} (<2 wt.% crystallinity) display higher INA than their counterpart LIP_{glass} and CID_{glass}, which could reflect the influence of minor crystalline components (below quantification by XRD; Table 2) in these tephra on their ability to nucleate ice. However, the difference between tephra and glass $T_{n_s \approx 1\ cm^{-2}}$ values across the nine sample pairs ($\Delta T_{n_s \approx 1\ cm^{-2}}$, ranging from ~2 to 19 °C) does

not vary simply with respect to tephra crystallinity (<2 to 66 wt.%; Fig. S1a). Additionally, a plot of $T_{n_s \approx 1\ cm^{-2}}$ values versus crystallinity of the tephra samples shows no correlation between ice nucleation and crystalline content (Fig. S1b). The compositionally quite similar NUO_{teph} and AST_{teph} display the highest IN~~E~~A ($T_{n_s \approx 1\ cm^{-2}}$ values of -5.0 and -6.4 °C, respectively) and are characterised by markedly contrasting crystallinities (60 and 28 wt.%, respectively). A difference in crystallinity was proposed as one of a number of potential explanations for the variable IN~~E~~A of two ash samples from Soufrière Hills volcano~~, Montserrat~~, with the 100% crystalline material produced by a dome collapse showing a higher IN~~E~~A than the 89% crystalline material produced by a magmatic eruption (Schill et al., 2015; Mangan et al., 2017). However, in light of our findings, it seems unlikely that this slight difference in crystallinity of two Soufrière Hills ash samples can adequately explain the large disparity in their IN~~E~~A.

A study comparing ice nucleation by crystalline and glassy anorthite ($CaAl_2Si_2O_8$), with the former displaying a $n_s(T)$ curve reaching higher freezing temperatures than the latter, suggested that crystals may introduce rarer, more ice-active surface sites but are not required for ice nucleation (Harrison et al., 2016). ~~In addition, aqueous organic solutions in a glassy state have been shown to nucleate ice (Murray et al., 2010b; Wagner et al., 2012; Ignatius et al., 2016).~~ In contrast, our observations strongly suggest that the presence of crystals is crucial in making volcanic ash an effective ice nucleant, although the abundance of crystalline phases in ash may be less important than the mere presence and specific properties of those phases in determining the IN~~E~~A.

4.2 Mineralogy

Consideration of the nine tephra samples m~~ight~~ay provide insight into the influence of mineralogy on the IN~~E~~A of volcanic ash. As noted above, comparison of the compositionally analogous tephra-glass pairs points to a role of crystalline phases in promoting freezing, and we infer that the properties of those phases have a strong effect on a sample's IN~~E~~A. A study of ash from ~~Fuego,~~ Soufrière Hills, Fuego, and Taupo volcanoes attributed differences in their IN~~E~~A to their contrasting mineralogies (Schill et al., 2015). More recently, Jahn et al. (2019) proposed that feldspar and pyroxene were responsible for ice nucleation by ash from Soufrière Hills, Fuego, and Santiaguito volcanoes. Overall, when the $T_{n_s \approx 1\ cm^{-2}}$ values are plotted against the content of various minerals in the tephra samples studied here, no clear correlations are evident (Fig. 4). However, certain features do stand out; the two most ice-active NUO_{teph} and AST_{teph} have the highest contents of alkali feldspar (60 and 19 wt.%, respectively; Fig. 4a), while the next most ice-active COL_{teph} and TUN_{teph} are characterised by an abundance of plagioclase feldspar (55 and 43 wt.%, respectively; Fig. 4b) and lesser amounts of orthopyroxene (7 and 5 wt.%, respectively, Fig. 4d).

The $n_s(T)$ curves of our tephra samples are compared with the ~~ice-nucleating activity~~INA of ~~the two feldspar mineral groups~~ alkali (K-) and plagioclase (separated into Na-/Ca- and Na-) feldspars in Fig. 5. The $n_s(T)$ curves of NUO_{teph} and AST_{teph} span temperatures consistent with the ~~alkali~~ K-feldspar parameterisation compiled from literature data (Harrison et al., in prep.), supporting the notion that the IN~~E~~A of these two samples relates to the presence of this mineral phase. The next two most ice-active materials COL_{teph} and TUN_{teph} contain no appreciable quantity of alkali feldspar, instead being rich in plagioclase feldspar. However, the $n_s(T)$ curves of these two samples are inconsistent with the relatively low IN~~E~~A of ~~plagioclase~~ Na-/Ca-feldspar reported in the literature (Fig. 5). This may point to the presence in COL_{teph} and TUN_{teph} of ~~very~~ ice-active plagioclase feldspar characterised by an INA closer to the Na-feldspar (albite) parameterisation, or potentially more akin to the hyper-active feldspars measured by Harrison et al. (2016; Fig. 5).~~or to the influence of some other component in COL_{teph} and TUN_{teph} (e.g., orthopyroxene, discussed below). Harrison et al. (2016) have found that some alkali and plagioclase feldspar samples are hyper-active relative to the majority of materials tested, hence our observations may simply reflect the natural variability in INE of feldspar minerals.~~ It is not clear why these hyper-active samples (Amelia albite and TUD#3 microcline) have a much

greater INA relative to the majority of feldspars tested (Harrison et al., 2016; Peckhaus et al., 2016), but such wide variability may relate to the specific mechanisms and/or conditions of formation and subsequent processing of individual samples (Welti et al., 2019), and it might be that plagioclase feldspar in COL_{teph} and TUN_{teph} was produced in a way that gives rise to enhanced activity. Alternatively, the high INA of these two tephra samples may relate to the influence of some other mineral component such as orthopyroxene; this possibility is discussed in more detail below.

Other tephra samples containing feldspar are comparatively less effective at nucleating ice, in particular; the intermediately ice-active ETN_{teph} (44 wt.% plagioclase feldspar; Fig. 4b) and the least ice-active KIL_{teph} (3 wt.% plagioclase feldspar; Fig. 4b) and LAC_{teph} (9 wt.% alkali feldspar; Fig. 4a). Such differences m~~ay~~ight relate to the specific chemistry of the mineral phases present in the tephra (Zolles et al., 2015; Welti et al., 2019). Harrison et al. (2016) showed that the IN~~E~~A of feldspar generally decreases from the K end-member ($KAlSi_3O_8$) to the Na end-member ($NaAlSi_3O_8$) to the Ca end-member ($CaAl_2Si_2O_8$), with the exception of a hyper-active ~~$NaAlSi_3O_8$~~ Amelia albite specimen (~~Amelia albite~~Fig. 5). Based on electron microprobe analysis (Text S1, Table S2), the Na_2O/CaO ratio in plagioclase feldspar in COL_{teph} and TUN_{teph} (both ~0.5) is higher than in ETN_{teph} and KIL_{teph} (both ~0.2), reflecting a greater proportion of the more ice-active $NaAlSi_3O_8$ relative to $CaAl_2Si_2O_8$ in the former samples. On the other hand, the K_2O/Na_2O ratio in alkali feldspar in NUO_{teph}, AST_{teph} and LAC_{teph} (1.2, 5.0, 1.9, respectively) does not support a link between these samples' IN~~E~~A and the proportion of $KAlSi_3O_8$ relative to $NaAlSi_3O_8$. This is consistent with the results of Whale et al. (2017), who found that the IN~~E~~A of alkali feldspar does not relate directly to K content, but rather to the presence of perthitic intergrowth microtexture arising from phase separation (exsolution) into Na- and K-rich regions. Strain at the boundary of these regions gives rise to nanoscale topographic features that are suggested to be important in generating sites for ice nucleation (Whale et al., 2017; Holden et al., 2019). It may be that these features stabilise patches of the high-energy (100) crystallographic plane exposed by surface defects, which Kiselev et al. (2017) showed to be favourable sites for ice nucleation on alkali feldspar.

However, ~~P~~perthite in alkali feldspar develops in metamorphic and plutonic contexts during slow cooling at temperatures <700 °C (Parsons, 2010), and is generally not expected in volcanic ash which cools rapidly from magmatic down to ambient temperatures during eruption (Parsons et al., 2015). An absence of perthitic microtexture is consistent with ~~T~~the low IN~~E~~A of LAC_{teph} in spite of its alkali feldspar content (9 wt.%). ~~could hence reflect a lack of perthitic microtexture, as noted for the~~This is supported by evidence that the alkali feldspar mineral sanidine ~~($KAlSi_3O_8$)~~ sourced from the same geological setting as LAC_{teph} (Eifel volcanic field) lacks perthitic texture and exhibits ~~, and similarly showing~~ a poor ability to nucleate ice (Whale et al., 2017). A recent study similarly found volcanic sanidine from Germany to be the least ice-active among the alkali feldspar samples tested (Welti et al., 2019). In contrast, an absence of perthitic microtexture is inconsistent with the high IN~~E~~A of NUO_{teph} and AST_{teph} ~~is surprising in the absence of perthitic microtexture~~, and perhaps some other textural feature underlies the~~ir~~ samples' ability to nucleate ice as effectively as alkali feldspar of non-pyroclastic origin (Fig. 5). Pyroclastic material from both the 1538 Monte Nuovo eruption (i.e., the origin of NUO_{teph}) and the ~4 ka Astroni eruption (i.e., the origin of AST_{teph}) has been found to contain anti-rapakivi overgrowth microtexture characterised by plagioclase feldspar cores rimmed by alkali feldspar (D'Oriano et al., 2005; Astbury et al., 2016; 2018). We are not aware of any studies reporting similar textures in pyroclastic material from the 12.9 ka Laacher See eruption (i.e., the origin of LAC_{teph}). Such textures are challenging to resolve optically in powdered samples including the tephra studied here. Further optical and microanalytical (Scanning- and Transmission Electron Microscopy) observations (e.g., Whale et al., 2017; Holden et al., ~~in press~~2019) will be needed to explore whether the boundary between Na- and K-rich regions in anti-rapakivi microtexture may give rise to nanoscale topography that induces effects analogous to perthitic microtexture in promoting ice nucleation.

In addition to feldspar, several of the tephra samples contain pyroxene (Table 2), an aluminosilicate mineral group of the general formula XYZ_2O_6, where X and Y are often Mg^{2+}, Fe^{2+} or Ca^{2+} and Z is Si^{4+} or sometimes Al^{3+} (Morimoto et al., 1988). A solid solution exists between the $Mg_2Si_2O_6$ and $Fe_2Si_2O_6$ end-members with small amounts of Ca^{2+} substitution possible

(orthopyroxenes), whereas solid immiscibility occurs between other compositions particularly with higher Ca^{2+} content (clinopyroxenes). ~~Specifically, t~~The presence of orthopyroxene distinguishes COL_{teph} and TUN_{teph} from the other tephra (Fig. 4d), raising the question of whether it may underlie the high IN~~E~~A of these two samples (i.e., rather than plagioclase feldspar). We are aware of ~~only~~ a few early studies on ice nucleation by ortho- and clinopyroxene minerals (hypersthene, augite; Hama and Itoo, 1956; Isono and Ikebe, 1960), but these studies ~~have~~ only report~~ed~~ semi-quantitative onset freezing temperatures (between -8 and -15 °C). More recently, Jahn et al. (2019) measured the INA of a clinopyroxene specimen (freezing from -8 to -24 °C), citing its behaviour to explain the INA of three pyroxene-containing volcanic ash samples. However, XRD analysis indicated that this specimen comprising diopside-augite also contained ~5 wt.% feldspar, which might have influenced the INA observed. In any case, it should be emphasised that a single mineral specimen might not provide a good representation of the INA of a given mineral type, as shown by studies on ice nucleation by feldspar and quartz (Harrison et al., 2016; Whale et al., 2017; Harrison et al., in prep.). Therefore, at present we cannot rule out a potential influence of pyroxene ~~minerals~~ on ice nucleation by volcanic ash. Additional research is needed to quantify the IN~~E~~A of a range of pyroxene minerals, and probe the nature of their ice-nucleating properties, in order to better inform this assessment.

4.3 Chemical composition

To explore a potential link between chemical composition and IN~~E~~A, the $T_{n_s \approx 1\ cm^{-2}}$ values of the tephra and glass samples are plotted as a function of SiO_2, Al_2O_3, Fe_2O_3, MgO, CaO, Na_2O, K_2O, TiO_2, MnO and P_2O_5 contents in Fig. S2. No clear correlations are observed in any of these scatter plots to indicate a compositional dependency of the tephra or glass IN~~E~~A. This stands in apparent contrast to the recent work of Genareau et al. (2018) (based on a sample set of two rhyolites and three basalts), who reported that the $n_s(T)$ of volcanic ash correlates positively with K_2O content at -25 °C and negatively with TiO_2 and MnO contents from -30 to -35 °C.

The glass samples, in lacking crystalline minerals, are well-suited to assess for any direct relationships between IN~~E~~A and specific element oxide abundances. However, due to the overlap of droplet freezing temperatures of the glass suspensions and the background water (Fig. 2b), our ability to distinguish differences in IN~~E~~A across the nine samples is impeded. While CID_{glass} and COL_{glass} are the most ice-active glass samples, with signals clearly above the background (Fig. 2b, d), they represent intermediate chemical compositions and thus their behaviour does not support any simple link between ash IN~~E~~A and chemical composition. It is possible that CID_{glass} and COL_{glass} contain very small amounts of crystals below detection by XRD that survived melting or formed during quenching, which could explain why these glasses stand out in their ability to nucleate ice.

In contrast, the tephra samples are characterised by variations in crystallinity and mineralogy as well as composition, which convolutes the assessment of relationships between IN~~E~~A and specific element oxide abundances. However, if the crystallinity and mineralogy of the tephra samples are taken into consideration, a broad pattern emerges in the plots of $T_{n_s \approx 1\ cm^{-2}}$ versus Fe_2O_3, MgO, and CaO contents (Fig. S2c-e). Excluding a cluster of three samples with comparatively low crystallinities (LIP_{teph}, CID_{teph}, LAC_{teph}), the $T_{n_s \approx 1\ cm^{-2}}$ decreases with increasing Fe_2O_3, MgO, and CaO contents for NUO_{teph}, AST_{teph}, COL_{teph}, TUN_{teph}, ETN_{teph}, and KIL_{teph} (Fig. 6), in an order consistent with interpretations relating to their feldspar contents and chemistries and/or a potential effect of orthopyroxene in two of these samples (see discussion Sect. 4.2). This conforms to the notion of an indirect relationship between chemical composition and volcanic ash IN~~E~~A, whereby FeO/Fe_2O_3, MgO, and CaO contents increase from felsic to mafic magma, influencing the mineral phases that can crystallise from the magma and hence exist in the resultant ash (Fig. 1b).

5 Conclusions and implications

Here we used nine compositionally analogous pairs of natural tephra and remelted and quenched glass to investigate the influence of chemical composition, crystallinity and mineralogy on the IN~~E~~A of volcanic ash. The higher IN~~E~~A of the tephra relative to the glass strongly suggests that the presence of crystalline phases promotes ice nucleation. The large variability in IN~~E~~A of the tephra is inferred to reflect an influence of mineralogy - and hence an indirect influence of magma composition - on ice nucleation. As in desert dust, alkali feldspar is probably the most ice-active component in volcanic ash, conferring the highest IN~~E~~A to NUO_{teph} and AST_{teph} in this study. However, the ability of alkali feldspar in ash to nucleate ice likely cannot unequivocally be attributed to perthitic microtexture, as has been done for alkali feldspar of non-pyroclastic origin. Additional research is needed to explore whether other textural features in ash may elicit a similar effect in promoting ice nucleation. Further, the presence of alkali feldspar is neither always sufficient nor necessary for effective ice nucleation by ash. The high IN~~E~~A of COL_{teph} and TUN_{teph} may alternatively reflect very ice-active plagioclase feldspar, or possibly orthopyroxene, which is present exclusively in these studied tephras. Previous studies on Soufrière Hills ash, also lacking alkali feldspar and containing plagioclase feldspar and orthopyroxene, have reported ~~both a~~ low ~~and~~ to high IN~~E~~A of this ash (Schill et al., 2015; Mangan et al., 2017; Jahn et al., 2019). Future studies quantifying the IN~~E~~A of individual crystalline phases found in ash will be necessary to unravel the precise role of mineralogy in volcanic ash ice nucleation.

An improved knowledge of the link between particular ash properties and ash IN~~E~~A may ultimately enhance predictive capability regarding volcanic eruptions likely to generate ice-active material. For example, as crystalline phases are primarily controlled by magma composition and storage/ascent conditions (Rogers, 2015), we speculate that highly ice-active ash particles might be erupted by volcanoes with intermediate to felsic alkaline magmas ~~*and* possessing a history of magma mixing leading to~~giving rise to feldspar crystals featuring overgrowth textures (e.g., Astbury et al., 2016; 2018) or potentially pyroxene crystals with high INA for reasons yet unknown (e.g., Jahn et al., 2019). In addition, an eruption producing an abundance of crystal-bearing particles is expected to elicit a greater impact on heterogeneous ice nucleation than an eruption producing an abundance of crystal-free glass particles, all else being equal. Accordingly, massive outputs from the largest and most explosive eruptions, corresponding to violent caldera-forming ignimbrite events that generate ash clouds dominated by the glassy component (Sparks et al., 1997; Cather et al., 2009), m~~ay~~ight be less efficient in affecting INP populations than ash emissions from smaller eruptions. Further, since airborne ash typically becomes enriched in glassy fragments during long-range transport due to earlier gravitational settling of crystalline fragments (Hinkley et al., 1982), the IN~~E~~A of a suspended ash population is expected to decrease over time and distance from the volcano.

Lastly, it must be noted that once ash particles are generated, their surface properties can be altered by interactions with gases and condensates (e.g., H_2O, SO_2, H_2SO_4, HCl, HF) at variable temperatures in the eruption plume/cloud and ambient atmosphere (Delmelle et al., 2007; Ayris et al., 2013; 2014; Maters et al., 2016; 2017). The effects of such interactions on ash IN~~E~~A are not known, although it has been suggested from field measurements that volcanic gases may deactivate INPs (Schnell and Delany, 1976; Schnell et al., 1982). Laboratory studies on desert dust show that 'aging' of dust particle surfaces by exposure to H_2SO_4 vapours at elevated temperatures reduces dust IN~~E~~A, possibly by destroying ice-active surface sites (Sullivan et al., 2010; Niedermeier et al., 2011). Moreover, it has recently been shown that even very low concentrations of soluble salts (~10^{-4} M) can influence the INA of feldspar minerals (Kumar et al., 2018; Whale et al., 2018), and we cannot exclude the possibility that small amounts of NaCl or KCl formed by prior ash-gas/condensate interactions in our tephra samples reduced their INA. However, given the strong correlations observed between INA and composition of the crystalline tephra samples (Fig. 6), we do not think that a potential influence of soluble salts on freezing temperatures affects the general conclusions of this study. ~~Therefore, e~~Exploring such potential eruptive and atmospheric controls on ash IN~~E~~A is an important next step towards developing a better understanding of the capacity of volcanic ash emissions to affect heterogeneous ice nucleation during their airborne lifetime.

Data availability: e.c.maters@leeds.ac.uk

Author contribution: E.M. designed the study and carried out the experiments. D.D. and C.C. provided the tephra samples and produced the glass samples. D.M. performed chemical and mineralogical analyses of these samples. T.W. performed the Poisson Monte Carlo error calculations. B.M supervised the project and provided insight on data interpretation. E.M. wrote the manuscript with contributions from all co-authors.

Competing interests: The authors declare that they have no conflict of interest.

Acknowledgements: E.M. is funded by the European Union's Horizon 2020 Research and Innovation Programme under the Marie Skłodowska-Curie Actions grant agreement No. 746695 (INoVA project). B.M. also acknowledges the European Research Council (MarineIce: No. 648661; CryoProtect: No. 713664) for funding. The authors wish to thank Ulrich Küppers for collecting many of the tephra samples used in this study, and Bruce Houghton who made possible the collection of Kilauea achneliths. We also thank Nora Groschopf (Institute of Geosciences, Johannes Gutenberg University Mainz) for XRF analyses of our samples. We are also grateful to William Orsi for enabling access to ultrapure water facilities at LMU, Alex Harrison for providing the plagioclase and alkali feldspar parameterisations, and to Sebastien Sikora, Lesley Neve, Fiona Keay and Andy Connelly for laboratory assistance.

References

Astbury, R. L., Petrelli, M., Arienzo, I., D'Antonio, M., Morgavi, D., and Perugini, D.: Using trace element mapping to identify discrete magma mixing events from the Astroni 6 eruption, in: American Geophysical Union Fall Meeting 2016, San Francisco, United States of America, 12-16 December 2016, 2016AGUFM.V33E3176A, 2016.

Astbury, R. L., Petrelli, M., Ubide, T., Stock, M. J., Arienzo, I., D'Antonio, M., and Perugini, D.: Tracking plumbing system dynamics at the Campi Flegrei caldera, Italy: High-resolution trace element mapping of the Astroni crystal cargo, Lithos, 318-319, 464-477, https://doi.org/10.1016/j.lithos.2018.08.033, 2018.

Atkinson, J. D., Murray, B. J., Woodhouse, M. T., Whale, T. F., Baustian, K. J., Carslaw, K. S., Dobbie, S., O'Sullivan, D., and Malkin, T. L.: The importance of feldspar for ice nucleation by mineral dust in mixed-phase clouds, Nature, 498, 355-358, doi:10.1038/nature12278, 2013.

Ayris, P. M., Lee, A. F., Wilson, K., Kueppers, U., Dingwell, D. B., and Delmelle, P.: SO_2 sequestration in large volcanic eruptions: high-temperature scavenging by tephra, Geochim. Cosmochim. Ac., 110, 58-69, https://doi.org/10.1016/j.gca.2013.02.018, 2013.

Ayris, P. M., Delmelle, P., Cimarelli, C., Maters, E. C., Suzuki, Y. J., and Dingwell, D. B.: HCl uptake by volcanic ash in the high temperature eruption plume: Mechanistic insights, Geochim. Cosmochim. Ac., 144, 188-201, https://doi.org/10.1016/j.gca.2014.08.028, 2014.

Brunauer, S., Emmett, P. H., and Teller, E.: Adsorption of gases in multimolecular layers, J. Am. Chem. Soc., 60, 309-319, doi:10.1021/ja01269a023, 1938.

Cather, S. M., Dunbar, N. W., McDowell, F. W., McIntosh, W. C., and Scholle, P. A.: Climate forcing by iron fertilization from repeated ignimbrite eruptions: The icehouse silicic large igneous province (SLIP) hypothesis, Geosphere, 5, 315−324, https://doi.org/10.1130/GES00188.1, 2009.

Cimarelli, C., Alatorre-Ibargüengoitia, M. A., Aizawa, K., Yokoo, A., Díaz-Marina, A., Iguchi, M., and Dingwell D. B.: Multiparametric observation of volcanic lightning: Sakurajima Volcano, Japan, Geophys. Res. Lett., 43, 4221-4228, https://doi.org/10.1002/2015GL067445, 2016.

Connolly, P. J., Möhler, O., Field, P. R., Saathoff, H., Burgess, R., Choularton, T., and Gallagher, M.: Studies of heterogeneous freezing by three different desert dust samples, Atmos. Chem. Phys., 9, 2805–2824, https://doi.org/10.5194/acp-9-2805-2009, 2009.

Delmelle, P., Lambert, M., Dufrêne, Y., Gerin, P., and Óskarsson, N.: Gas/aerosol-ash interaction in volcanic plumes: New insights from surface analysis of fine ash particles, Earth Planet Sc. Lett., 259, 159-170, https://doi.org/10.1016/j.epsl.2007.04.052, 2007.

Döbelin, N., and Kleeberg, R.: Profex: a graphical user interface for the Rietveld refinement program BGMN, J. Appl. Crystallogr, 48, 1573-1580, https://doi.org/10.1107/S1600576715014685, 2015.

D'Oriano, C., Poggianti, E., Bertagnini, A., Cioni, R., Landi, P., Polacci, M., and Rosi, M.: Changes in eruptive style during the A.D. 1538 Monte Nuovo eruption (Phlegrean Fields, Italy): the role of syn-eruptive crystallization, B. Volcanol., 67, 601-621, doi:10.1007/s00445-004-0397-z, 2005.

Durant, A. J., Shaw, R. A., Rose, W. I., Mi-, Y., and Ernst, G. G.: Ice nucleation and overseeding of ice in volcanic clouds, J. Geophys. Res., 113, D09206, https://doi.org/10.1029/2007JD009064, 2008.

Durant, A. J., Bonadonna, C., Horwell, C. J.: Atmospheric and environmental impacts of volcanic particulates, Elements, 6, 235-240, https://doi.org/10.2113/gselements.6.4.235, 2010.

Genareau, K., Cloer, S. M., Primm, K., Tolbert, M. A., and Woods, T. W.: Compositional and mineralogical effects on ice nucleation activity of volcanic ash, Atmosphere, 9, 238, https://doi.org/10.3390/atmos9070238, 2018.

Guo, S., Bluth, G. J. S., Rose, W. I., Watson, I. M., and Prata, A. J.: Re-evaluation of SO_2 release of the 15 June 1991 Pinatubo eruption using ultraviolet and infrared satellite sensors, Geochem. Geophy. Geosy., 5, Q04001, https://doi.org/10.1029/2003GC000654, 2004a.

Guo, S., Rose, W. I., Bluth, G. J. S., and Watson, I. M.: Particles in the great Pinatubo volcanic cloud of June 1991: The role of ice, Geochem. Geophy. Geosy., 5, Q05003, https://doi.org/10.1029/2003GC000655, 2004b.

Hama, K., and Itoo, K.: Freezing of supercooled water-droplets (II), Pap. Meteorol. Geophys., 7, 99-106, https://doi.org/10.2467/mripapers1950.7.2_99, 1956.

Harrison, A. D., Lever, K., Sanchez-Marroquin, A., Holden, M. A., Whale, T. F., Tarn, M. D., McQuaid, J. B., and Murray, B. J.: The ice- -nucleating ~~efficiency~~ ability of ~~a variety of~~ quartz ~~samples~~ immersed in water and ~~their~~its atmospheric importance compared to K-feldspar. In preparation for Atmos. Chem. Phys.

Harrison, A. D., Whale, T. F., Carpenter, M. A., Holden, M. A., Neve, L., O'Sullivan, D., Vergara Temprado, J., and Murray B. J.: Not all feldspars are equal: a survey of ice nucleating properties across the feldspar group of minerals, Atmos. Chem. Phys., 16, 10927-10940, https://doi.org/10.5194/acp-16-10927-2016, 2016.

Heiken, G., and Wohletz, K. (Eds.): Volcanic Ash, University of California Press, London, United Kingdom, 1992.

Hinkley, T. K., Smith, K. S., Taggart, J. E., and Brown, J. T.: Chemical and mineralogic aspects of observed fractionation of ash from May 18, 1980 eruption of Mount St. Helens, U.S. Geological Survey Professional Paper 1397-A, 10−22, 1982.

Hobbs, P. V., Fullerton, C. M., and Bluhm, G. C.: Ice nucleus storms in Hawaii, Nat. Phys., 230, 90-91, 10.1038/physci230090a0, 1971.

Holden, M. A., Whale, T. F., Tarn, M. D., O'Sullivan, D., Walshaw, R. D., Murray, B. J., Meldrum, F. C., and Christenson, H. K.: High-speed imaging of ice nucleation in water proves the existence of active sites, Sci.~~ence~~ Adv.~~ances~~, ~~in press.~~ 5, eaav4316, doi: 10.1126/sciadv.aav4316, 2019.

Hoose, C., Kristjánsson, J. E., Chen, J.-P., Hazra, A.: A classical-theory-based parameterization of heterogeneous ice nucleation by mineral dust, soot, and biological particles in a global climate model, J. Atmos. Sci., 67, 2483-2503, https://doi.org/10.1175/2010JAS3425.1, 2010.

Herzog, M., Graf, H. F., Textor, C., and Oberhuber, J. M.: The effect of phase changes of water on the development of volcanic plumes. J. Volcanol. Geoth. Res., 87, 55-74, https://doi.org/10.1016/S0377-0273(98)00100-0, 1998.

Ignatius, K., Kristensen, T. B., Järvinen, E., Nichman, L., Fuchs, C., Gordon, H., Herenz, P., Hoyle, C. R., Duplissy, J., Garimella, S., Dias, A., Frege, C., Höppel, N., Tröstl, J., Wagner, R., Yan, C., Amorim, A., Baltensperger, U., Curtius, J., Donahue, N. M., Gallagher, M. W., Kirkby, J., Kulmala, M., Möhler, O., Saathoff, H., Schnaiter, M., Tomé, A., Virtanen, A., Worsnop, D., and Stratmann, F.: Heterogeneous ice nucleation of viscous secondary organic aerosol produced from ozonolysis of α pinene. Atmos. Chem. Phys., 16, 6495-6509, https://doi.org/10.5194/acp-16-6495-2016, 2016.

Isono, K., and Ikebe, Y.: On the ice-nucleating ability of rock-forming minerals and soil particles, J. Meteorol. Soc. Jpn., 38, 213-230, https://doi.org/10.2151/jmsj1923.38.5_213, 1960.

Isono, K., and Komabayasi, M.: The influence of volcanic dust on precipitation, J. Meteorol. Soc. Jpn., 32, 345-353, https://doi.org/10.2151/jmsj1923.32.11-12_345, 1954.

Isono, K., Komabayasi, M., and Ono, A.: Volcanoes as a source of atmospheric ice nuclei. Nature, 183, 317-318, https://doi.org/10.1038/183317a0, 1959a.

Isono, K., Komabayasi, M., and Ono, A.: The nature and origin of ice nuclei in the atmosphere, J. Meteorol. Soc. Jpn., 37, 211-233, https://doi.org/10.2151/jmsj1923.37.6_2111, 959b.

Jahn, L., Fahy, W., Williams, D. B., and Sullivan, R. C.: The role of feldspar and pyroxene minerals in the ice nucleating ability of three volcanic ashes, ACS Earth Space Chem., XX, XX-XX, doi:10.1021/acsearthspacechem.9b00004, 2019.

Kaufmann, L., Marcolli, C., Hofer, J., Pinti, V., Hoyle, C. R., and Peter, T.: Ice nucleation efficiency of natural dust samples in the immersion mode, Atmos. Chem. Phys., 16, 11177-11206, https://doi.org/10.5194/acp-16-11177-2016, 2016.

Kiselev, A., Bachmann, F., Pedevilla, P., Cox, S. J., Michaelides, A., Gerthsen, D., and Leisner, T.: Active sites in heterogeneous ice nucleation – the example of K-rich feldspars, Science, 355, 367-371, doi:10.1126/science.aai8034, 2017.

Komabayasi, M.: The suppression of thunder cloud occurrence by frequent volcanic eruptions, J. Meteorol. Soc. Jpn., 35A, 25-30, https://doi.org/10.2151/jmsj1923.35A.0_25, 1957.

Koop, T., and Murray, B. J.: A physically constrained classical description of the homogeneous nucleation of ice in water, *Journal of Chemical Physics*, 145, 211915, 2016.

Kulkarni, G., Nandasiri, M., Zelenyuk, A., Beranek, J., Madaan, N., Devaraj, A., Shutthanandan, V., Thevuthasan, S., and Varga, T.: Effects of crystallographic properties on the ice nucleation properties of volcanic ash particles, Geophys. Res. Lett., 42, 3048-3055, https://doi.org/10.1002/2015GL063270, 2015.

Kumar, A., Marcolli, C., and Peter, T.: Ice nucleation activity of silicates and aluminosilicates in pure water and aqueous solutions. Part 3 – Aluminosilicates, Atmos. Chem. Phys. Discuss., https://doi.org/10.5194/acp-2018-1021, 2018.

Le Maitre, R. W., Streckeisen, A., Zanettin, B., Le Bas, M. J., Bonin, B., and Bateman, P. (Eds.) Igneous Rocks: A Classification and Glossary of Terms, Recommendations of the International Union of Geological Sciences Subcommission on the Systematics of Igneous Rocks, Cambridge University Press, Cambridge, United Kingdom, 2002.

Mangan, T. P., Atkinson, J. D., Neuberg, J. W., O'Sullivan, D., Wilson, T. W., Whale, T. F., Neve, L., Umo, N. S., Malkin, T. L., and Murray, B. J.: Heterogeneous ice nucleation by Soufriere Hills volcanic ash immersed in water droplets, *PloS ONE*, 12, e0169720, https://doi.org/10.1371/journal.pone.0169720, 2017.

Maters, E.C., Delmelle, P., Rossi, M.J., Ayris, P.M., and Bernard, A.: Controls on the surface chemical reactivity of volcanic ash investigated with probe gases, Earth Planet Sc. Lett., 450, 254-262, https://doi.org/10.1016/j.epsl.2016.06.044, 2016.

Maters, E.C., Delmelle, P., Rossi, M.J., and Ayris, P.M.: Reactive uptake of sulfur dioxide and ozone on volcanic glass and ash at ambient temperature, J. Geophys. Res. - Atmos., 122, 10077-10088, https://doi.org/10.1002/2017JD026993, 2017.

McNutt, S. R., and Williams, E. R.: Volcanic lightning: global observations and constraints on source mechanisms, B. Volcanol., 72, 1153–1167, doi: 10.1007/s00445-010-0393-4, 2010.

Morimoto, N., Fabries, J., Ferguson, A. K., Ginzburg, I. V., Ross, M., Seifert, F. A., and Zussman, J.: Nomenclature of pyroxenes, Miner. Petrol., 39, 55-76, https://doi.org/10.1007/BF01226262, 1988.

Murray, B. J., Broadley, S. L., Wilson, T. W., Bull, S. J., Wills, R. H., Christenson, H. K., and Murray, E. J.: Kinetics of homogeneous freezing of water, Phys. Chem. Chem. Phys., 12, 10380-10387, doi:10.1039/c003297b, 2010a.

Murray, B. J., Wilson, T. W., Dobbie, S., Cui, Z., Al Jumur, S. M. R. K., Möhler, O., Schnaiter, M., Wagner, R., Benz, S., Niemand, M., Saathoff, H., Ebert, V., Wagner, S., and Kärcher, B.: Heterogeneous nucleation of ice particles on glassy aerosols under cirrus conditions, Nat. Geosci., 3, 233-237, https://doi.org/10.1038/ngeo817, 2010b.

Murray, B. J., O'Sullivan, D., Atkinson, J. D., and Webb, M. E.: Ice nucleation by particles immersed in supercooled cloud droplets, Chem. Soc. Rev., 41, 6519-6554, doi:10.1039/c2cs35200a, 2012.

Niedermeier, D., Hartmann, S., Clauss, T., Wex, H., Kiselev, A., Sullivan, R. C., DeMott, P.J., Petters, M. D., Reitz, P., Schneider, J., Mikhailov, E., Sierau, B., Stetzer, O., Reimann, B., Bundke, U., Shaw, R. A., Buchholz, A., Mentel, T. F., and Stratmann, F.: Experimental study of the role of physicochemical surface processing on the IN ability of mineral dust particles, Atmos. Chem. Phys., 11, 11131-11144, https://doi.org/10.5194/acp-11-11131-2011, 2011.

Parsons, I.: Feldspars defined and described: a pair of posters published by the Mineralogical Society. Sources and supporting information, Mineral. Mag., 74, 529-551, https://doi.org/10.1180/minmag.2010.074.3.529, 2010.

Parsons, I., Fitz Gerald, J. D., Lee, M. R.: Routine characterization and interpretation of complex alkali feldspar intergrowths, Am. Mineral., 100, 1277-1303, https://doi.org/10.2138/am-2015-5094, 2015.

Peckhaus, A., Kiselev, A., Hiron, T., Ebert, M., and Leisner, T.: A comparative study of K-rich and Na/Ca-rich feldspar ice-nucleating particles in a nanoliter droplet freezing assay, Atmos. Chem. Phys., 16, 11477-11496, doi:10.5194/acp-16-11477-2016, 2016.

Penner, J. E., Andreae, M., Annegarn, H., Barrie, L., Feichter, J., Hegg, D., Jayaraman, A., Leaitch, R., Murphy, D., Nganga, J., and Pitari, G.: Aerosols, their direct and indirect effects, in: Climate Change 2001: The Scientific Basis, Contribution of Working Group I to IPCC, Cambridge University Press, Cambridge, United Kingdom, 290–347, 2001.

Polen, M., Brubaker, T., Somers, J., and Sullivan, R. C.: Cleaning up our water: reducing interferences from non-homogeneous freezing of "pure" water in droplet freezing assays of ice nucleating particles, Atmos. Meas. Tech., 11, 5315-5334, https://doi.org/10.5194/amt-11-5315-2018, 2018.

Pruppacher, H. R., and Klett, J. D. (Eds.) Microphysics of Clouds and Precipitation, Second Edition, Springer, Netherlands, 2010.

Rogers, N.: The Composition and Origin of Magmas, in: The Encyclopedia of Volcanoes, Second Edition, edited by: Sigurdsson, H., Houghton, B., McNutt, S. R., Rymer, H., and Stix, J., Academic Press, London, United Kingdom, 93-112, https://doi.org/10.1016/B978-0-12-385938-9.00004-3, 2015.

Rose, W. I., Gu, Y., Watson, M., Yu, T., Bluth, G. J. S., Prata, A. J., Krueger, A. J., Krotkov, N., Carn, S., Fromm, M. D., Hunton, D. E., Ernst, G. G. J., Viggiano, A. A., Miller, T. M., Ballenthin, J. O., Reeves, J. M., Wilson, J. C., Anderson, B. E., and Flittner, D. E.: The February-March 2000 Eruption of Hekla, Iceland from a Satellite Perspective, in: Volcanism and the Earth's Atmosphere, Volume 139, edited by: Robock A., and Oppenheimer, C., American Geophysical Union, United States of America, 107-132, https://doi.org/10.1029/139GM07, 2003.

Schill, G. P., Genareau, K., and Tolbert, M. A.: Deposition and immersion-mode nucleation of ice by three distinct samples of volcanic ash, Atmos. Chem. Phys., 15, 7523-7536, https://doi.org/10.5194/acp-15-7523-2015, 2015.

Schnell, R. C., and Delany, A. C.: Airborne ice nuclei near an active volcano, Nature, 264, 535-536, https://doi.org/10.1038/264535a0, 1976.

Schnell, R. C., Pueschel, R. F., and Wellman, D. L.: Ice nucleus characteristics of Mount St. Helens effluents, J. Geophys. Res., 87, 11109-11112, https://doi.org/10.1029/JC087iC13p11109, 1982.

Seifert, P., Ansmann, A., Groß, S., Freudenthaler, V., Heinold, B., Hiebsch, A., Mattis, I., Schmidt, J., Schnell, F., Tesche, M., Wandinger, U., and Wiegner, M.: Ice formation in ash-influenced clouds after the eruption of the Eyjafjallajökull volcano in April 2010, J. Geophys. Res., 116, D00U04, https://doi.org/10.1029/2011JD015702, 2011.

Sparks, R. S. J., Bursik, M. I., Carey, S. N., Gilbert, J. S., Glaze, L. S., Sigurdsson, H., and Woods, A. W.: Volcanic Plumes, John Wiley & Sons, University of California, United States of America, 1997.

Sullivan, R. C., Petters, M. D., DeMott, P. J., Kreidenweis, S. M., Wex, H., Niedermeier, D., Hartmann, S., Clauss, T., Stratmann, F., Reitz, P., Schneider, J., and Sierau, B.: Irreversible loss of ice nucleation active sites in mineral dust particles caused by sulphuric acid condensation, Atmos. Chem. Phys., 10, 11471-11487, https://doi.org/10.5194/acp-10-11471-2010, 2010.

Textor, C., Graf, H. -F., Herzog, M., and Oberhuber, J. M.: Injection of gases into the stratosphere by explosive volcanic eruptions, J. Geophys. Res., 108, 4606, https://doi.org/10.1029/2002JD002987, 2003.

Textor, C., Graf, H. -F., Herzog, M., Oberhuber, J. M., Rose, W. I., and Ernst, G. G. J.: Volcanic particle aggregation in explosive eruption columns. Part I: Parameterization of the microphysics of hydrometeors and ash, J. Volcanol. Geoth. Res., 150, 359-377, https://doi.org/10.1016/j.jvolgeores.2005.09.007, 2006.

Vali, G.: Interpretation of freezing nucleation experiments: singular and stochastic; sites and surfaces, Atmos. Chem. Phys., 14, 5271–5294, https://doi.org/10.5194/acp-14-5271-2014, 2014.

Van Eaton, A. R., Mastin, L. G., Herzog, M., Schwaiger, H. F., Schneider, D. J., Wallace, K. L., and Clarke, A. B.: Hail formation triggers rapid ash aggregation in volcanic plumes, Nat. Commun., 6, 7860, https://doi.org/10.1038/ncomms8860, 2015.

Vergara-Temprado, J., Murray, B. J., Wilson, T. W., O'Sullivan, D., Browse, J., Pringle, K. J., Ardon-Dryer, K., Bertram, A. K., Burrows, S. M., Ceburnis, D., DeMott, P. J., Mason, R. H., O'Dowd, C. D., Rinaldi, M., and Carslaw, K. S.: Contribution of feldspar and marine organic aerosols to global ice nucleating particle concentrations, Atmos. Chem. Phys., 17, 3637-3658, https://doi.org/10.5194/acp-17-3637-2017, 2017.

Welti, A., Lohmann, U., and Kanji, Z. A.: Ice nucleation properties of K-feldspar polymorphs and plagioclase feldspars, Atmos. Chem. Phys. Discuss., https://doi.org/10.5194/acp-2018-1271, 2019.

Whale, T. F., Murray, B. J., O'Sullivan, D., Wilson, T. W., Umo, N. S., Baustian, K. J., J. D. Atkinson, J. D., Workneh, D. A., and Morris, G. J.: A technique for quantifying heterogeneous ice nucleation in microlitre supercooled water droplets, Atmos. Meas. Tech., 8, 2437-2447, https://doi.org/10.5194/amt-8-2437-2015, 2015.

Whale, T. F., Holden, M. A., Kulak, A. N., Kim, Y.-Y., Meldrum, F. C., Christenson, H. K., and Murray, B. J.: The role of phase separation and related topography in the exceptional ice-nucleating ability of alkali feldspars, Phys. Chem. Chem. Phys., 19, 31186-31193, doi:10.1039/c7cp04898j2, 2017.

Whale, T. F., Holden, M. A., Wilson, T. W., O'Sullivan D., and Murray, B. J.: The enhancement and suppression of immersion mode heterogeneous ice-nucleation by solutes, Chem. Sci., 9, 4142-4151, doi:10.1039/c7sc05421a, 2018.

~~Wagner, R., Möhler, O., Saathoff, H., Schnaiter, M., Skrotzki, J., Leisner, T., Wilson, T. W., Malkin, T. L., Murray, B. J.: Ice cloud processing of ultra-viscous/glassy aerosol particles leads to enhanced ice nucleation ability, Atmos. Chem. Phys., 12, 8589-8610, https://doi.org/10.5194/acp-12-8589-2012, 2012.~~

Wright, H. M. N., Cashman, K. V., Mothes, P. A., Hall, M. L., Ruiz, A. G., and Le Pennec, J.-L.: Estimating rates of decompression from textures of erupted ash particles produced by 1999–2006 eruptions of Tungurahua volcano, Ecuador, Geology, 40, 619-622, https://doi.org/10.1130/G32948.1, 2012.

Yakobi-Hancock, J. D., Ladino, L. A., and Abbat, J. P. D.: Feldspar minerals as efficient deposition ice nuclei, Atmos. Chem. Phys., 13, 11175-11185, https://doi.org/10.5194/acp-13-11175-2013, 2013.

Zolles, T., Burkart, J., Häusler, T., Pummer, B., Hitzenberger, R., and Grothe, H.: Identification of ice nucleation active sites on feldspar dust particles, J. Phys. Chem. A, 119, 2692-2700, doi:10.1021/jp509839x, 2015.

Table 1. Details of the volcanic tephra and glass samples used in this study.

Sample code	Source volcano	Eruption date[a]	Classification[b]	SSA_{BET}[c] (tephra/glass) ($m^2\ g^{-1}$)
$LIP_{teph/glass}$	Lipari (Italy)	1230	rhyolite	1.8/1.1
$COL_{teph/glass}$	Colima (Mexico)	Jan-Feb 2017	andesite	1.9/0.9
$TUN_{teph/glass}$	Tungurahua (Ecuador)	Feb 2014	andesite	1.4/1.1
$CID_{teph/glass}$	Sete Cidades (Portugal)	16 ka	trachyte	1.6/1.4
$AST_{teph/glass}$	Astroni (Italy)	3.8-4.4 ka	trachyphonolite	3.7/1.4
$NUO_{teph/glass}$	Monte Nuovo (Italy)	Sept-Oct 1538	trachyphonolite	4.6/1.3
$LAC_{teph/glass}$	Laacher See (Germany)	12.9 ka	phonolite	3.3/0.9
$ETN_{teph/glass}$	Mount Etna (Italy)	July 2014	trachybasalt	1.7/1.1
$KIL_{teph/glass}$	Kilauea (Hawaii)	July 2018	basalt	2.1/1.1

[a]Refers to the eruption of origin of the tephra material. This does not apply to the glass material as it has been synthesised (from tephra) in the laboratory by a melting, homogenising and quenching protocol. [b]According to the Total Alkali versus Silica igneous rock classification diagram (Fig. 1) based on chemical composition (Table S1). [c]Uncertainty is in the range of 0.5-1.2 %.

Table 2. Crystallinity and mineralogy of the tephra samples used in this study, in wt.%.

Sample[a]	Crystallinity	Alkali (K-rich) feldspar	Plagioclase (Na-/Ca-rich) feldspar	Clino-pyroxene	Ortho-pyroxene	Quartz	Fe(-Ti) oxide	Olivine
LIP_{teph}	<2	-	-	-	-	-	m.c.	-
COL_{teph}	62	m.c.	55	-	7	m.c.	m.c.	-
TUN_{teph}	54	-	43	6	5	-	m.c.	-
CID_{teph}	<2	m.c.	-	m.c.	-	-	m.c.	-
AST_{teph}	28	19	7	2	-	-	m.c.	-
NUO_{teph}	60	60	-	-	-	-	m.c.	-
LAC_{teph}	11	9	-	-	-	2	-	-
ETN_{teph}	66	-	44	22	-	-	m.c.	-
KIL_{teph}	3	-	3	-	-	-	-	m.c.

[a]Sample codes are listed in Table 1. m.c. = minor component; below ~2 wt.% ~~detection~~ quantification limit by XRD.

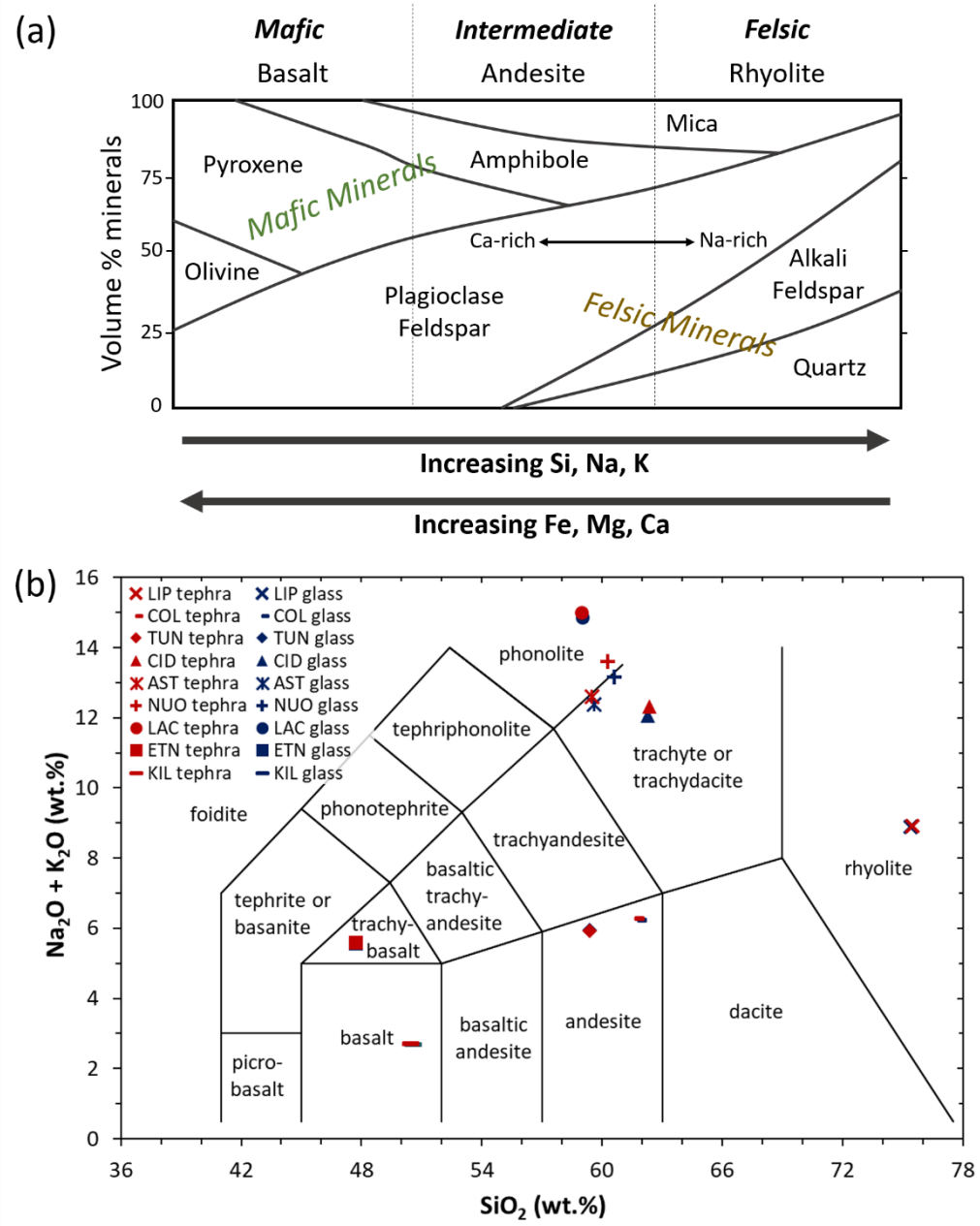

Figure 1. (a) Schematic summarising the mineralogy of common igneous rock types. Modified after Rogers (2015). (b) Total Alkali versus Silica diagram showing the classification of the tephra (red symbols) and glass (blue symbols) used in this study. Sample codes are listed in Table 1. Modified after Le Maitre et al. (2002). ~~(b) Schematic summarising the mineralogy of common igneous rock types. Modified after Rogers (2015).~~

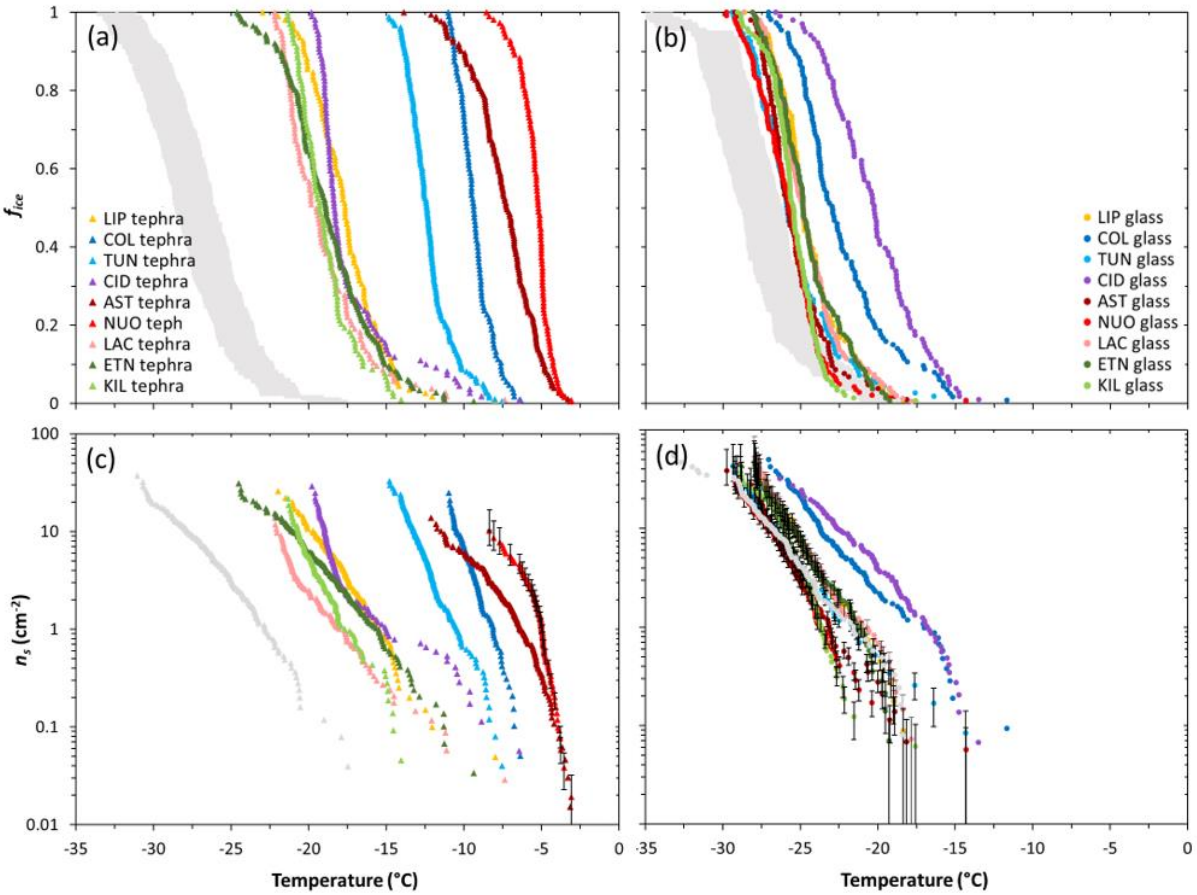

Figure 2. Droplet fraction frozen (f_{ice}) as a function of temperature for 1 wt.% suspensions of (a) tephra or (b) glass in water. The grey bands represent the spread of $f_{ice}(T)$ measurements (mean values ± standard deviation) of the background water (i.e., containing no added sample). Ice nucleation active site density (n_s) as a function of temperature for 1 wt.% suspensions of (c) tephra or (d) glass in water. For the sake of comparison, the grey curves represent theoretical upper limit $n_s(T)$ values of the background water, calculated using the upper limit $f_{ice}(T)$ measurements (mean values + standard deviation) of the background water, and assuming it contains particles with SSA_{BET} values equal to the lowest from the tephra and glass sets (1.4 and 0.9 m^2 g^{-1}, respectively). The tephra $n_s(T)$ values are well above this background but most of the glass $n_s(T)$ values should be regarded as upper limits. The uncertainty in $n_s(T)$ is shown as error bars for a subset of data points (of NUO_{teph} and ~~CID_{glass}~~LIP_{glass}, TUN_{glass}, AST_{glass}, NUO_{glass}, LAC_{glass}, ETN_{glass}, KIL_{glass}) and omitted from remaining data points for clarity, but is typical of all ~~tephra and glass~~ samples studied. Sample codes are listed in Table 1.

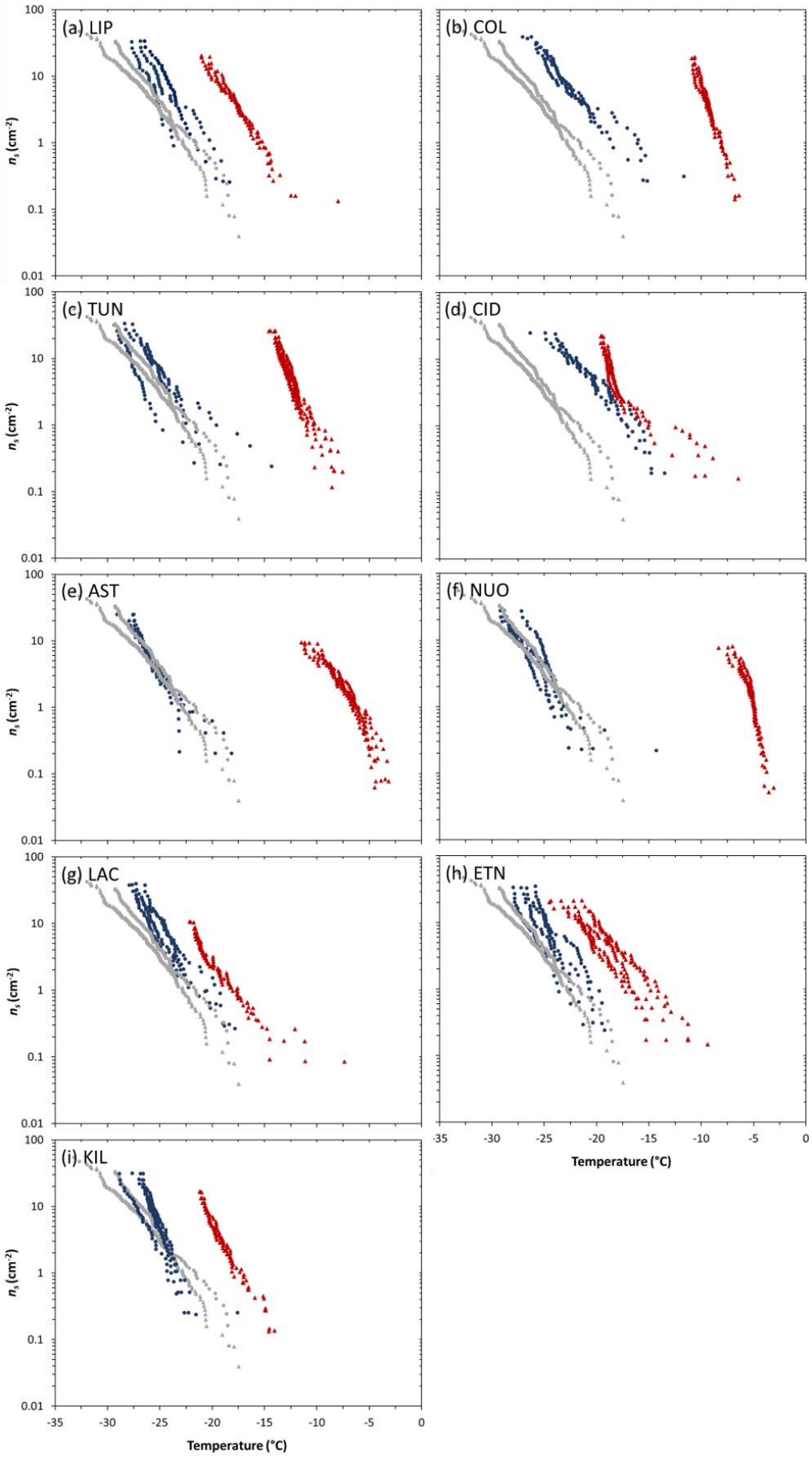

Figure 3. Ice nucleation active site density (n_s) as a function of temperature for 1 wt.% suspensions of tephra or glass in water. Each plot shows replicates of a compositionally analogous pair of tephra (red triangles) and glass (blue circles). The grey curves with triangle and circle symbols represent the detection limit for $n_s(T)$ based on the background water runs accompanying the tephra and glass experiments, respectively (see Fig. 2 caption for details). Sample codes are listed in Table 1.

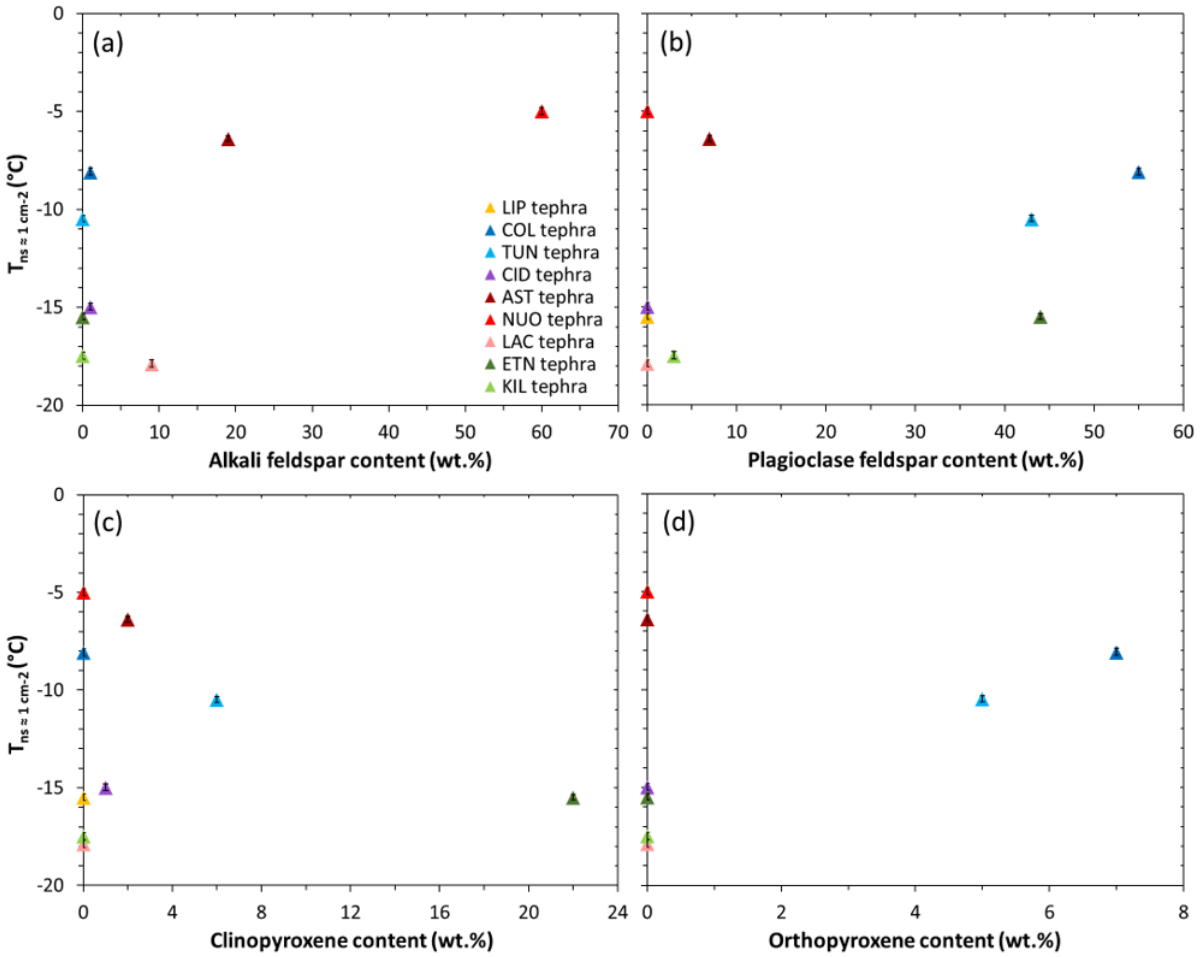

Figure 4. The IN~~E~~A ($T_{n_s \approx 1\ cm^{-2}}$) of the tephra versus their content of (a) alkali feldspar, (b) plagioclase feldspar, (c) clinopyroxene, and (d) orthopyroxene. Note that minor components below the XRD ~~detection~~ quantification limit are plotted at 1 wt.%. Ice nucleation experiments were conducted with 1 wt.% suspensions of tephra in water. The uncertainty in $T_{n_s \approx 1\ cm^{-2}}$ is shown as error bars (note that these are as small as the data symbols). Sample codes are listed in Table 1.

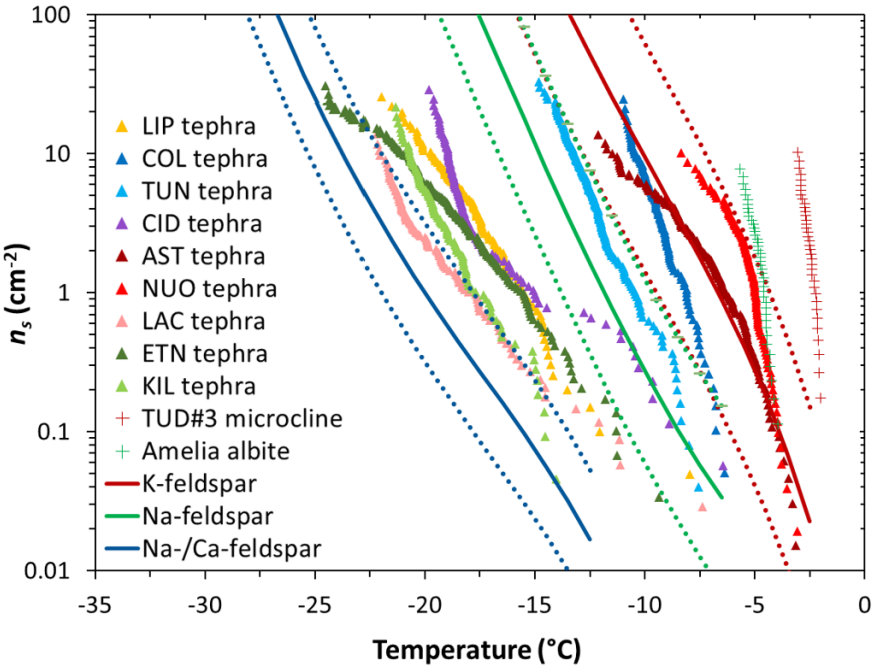

Figure 5. Ice nucleation active site density (n_s) as a function of temperature for 1 wt.% suspensions of tephra in water. Sample codes are listed in Table 1. The red and green crosses are the $n_s(T)$ values for, respectively, a hyper-active K-feldspar (TUD#3 microcline) and a hyper-active Na-feldspar (Amelia albite) measured by Harrison et al. (2016). The red, green, and blue ~~and red~~ lines represent parameterisations for, respectively, ~~alkali~~K-feldspar, Na-feldspar, and ~~plagioclase~~Na-/Ca- feldspar of non-pyroclastic origin reported in Harrison et al. (in prep.) from a compilation of literature data excluding the hyper-active feldspar specimens. The solid lines indicate mean values and the dashed lines indicate lower and upper limits corresponding to the standard deviation of the mean. ~~Sample codes are listed in Table 1.~~

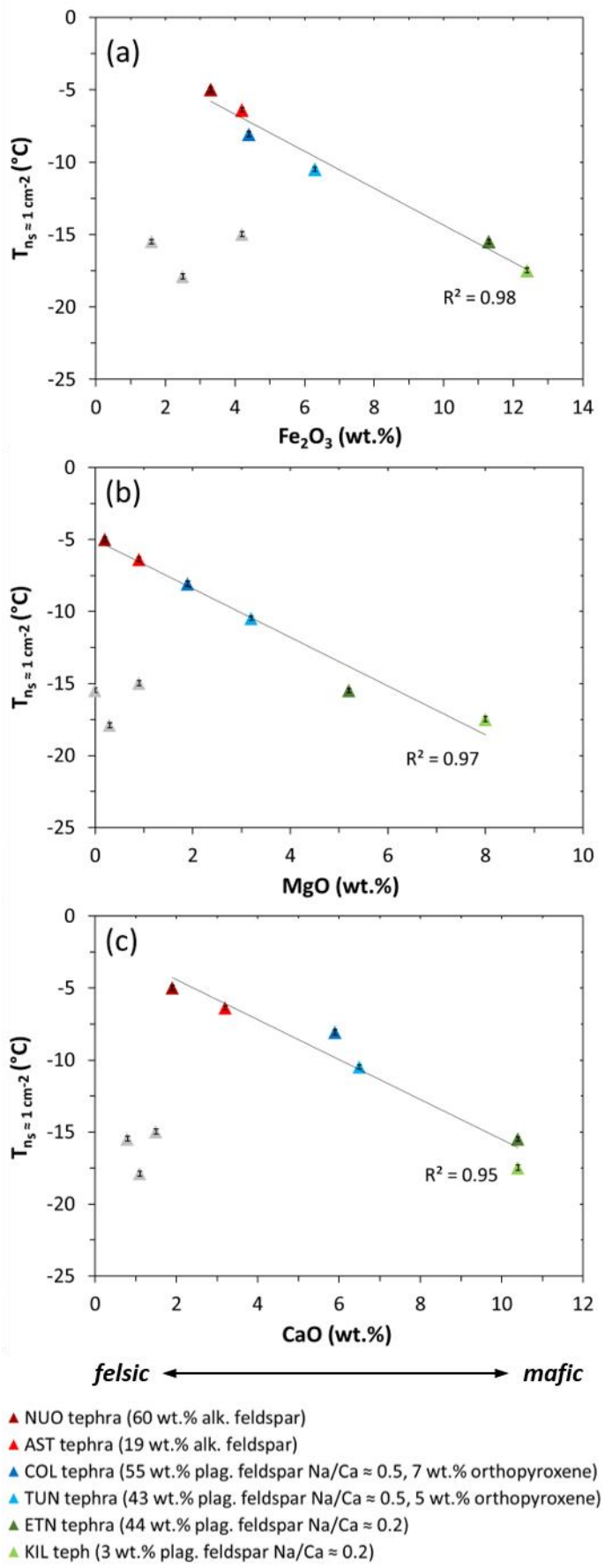

Figure 6. The IN~~E~~A ($T_{n_s \approx 1\ cm^{-2}}$) of NUO_{teph}, AST_{teph}, COL_{teph}, TUN_{teph}, ETN_{teph}, and KIL_{teph} versus their (a) Fe_2O_3, (b) MgO, and (c) CaO contents. The grey triangles correspond to tephra samples with comparatively low crystallinities (LIP_{teph}, CID_{teph}, LAC_{teph}) which are excluded from the trendline. Ice nucleation experiments were conducted with 1 wt.% suspensions of tephra in water. The uncertainty in $T_{n_s \approx 1\ cm^{-2}}$ is shown as error bars (note that these are as small as the data symbols). Sample codes are listed in Table 1.

Supplementary Material

Table S1. Bulk chemical composition of the tephra and glass samples used in this study, determined by X-ray fluorescence and normalised to 100 wt.% (excluding loss on ignition).

Sample[a]	SiO_2	Al_2O_3	Fe_2O_3	MgO	CaO	Na_2O	K_2O	TiO_2	MnO	P_2O_5
Tephra										
LIP_{teph}	75.5	13.0	1.6	0.0	0.8	3.7	5.2	0.1	0.1	0.0
COL_{teph}	61.7	18.9	4.4	1.9	5.9	4.9	1.4	0.5	0.1	0.2
TUN_{teph}	59.4	17.5	6.3	3.2	6.5	4.1	1.9	0.9	0.1	0.2
CID_{teph}	62.4	17.4	4.2	0.9	1.5	7.0	5.3	0.9	0.2	0.2
AST_{teph}	59.5	18.9	4.2	0.9	3.2	4.0	8.6	0.5	0.1	0.2
NUO_{teph}	60.3	19.9	3.3	0.2	1.9	6.4	7.2	0.4	0.2	0.0
LAC_{teph}	59.0	21.3	2.5	0.3	1.1	9.4	5.6	0.3	0.3	0.1
ETN_{teph}	47.7	17.3	11.3	5.2	10.4	3.6	2.0	1.7	0.2	0.6
KIL_{teph}	50.4	13.2	12.4	8.0	10.4	2.2	0.5	2.4	0.2	0.2
Glass										
LIP_{glass}	75.4	13.0	1.7	0.1	0.8	3.7	5.2	0.1	0.1	0.0
COL_{glass}	61.8	18.8	4.3	2.0	5.9	4.8	1.4	0.5	0.1	0.2
TUN_{glass}	59.4	17.5	6.3	3.2	6.5	4.1	1.9	0.9	0.1	0.2
CID_{glass}	62.3	17.4	4.4	0.9	1.7	6.9	5.2	0.9	0.2	0.2
AST_{glass}	59.6	18.9	4.2	0.9	3.2	3.9	8.5	0.5	0.1	0.2
NUO_{glass}	60.6	20.0	3.3	0.2	1.9	6.2	7.0	0.4	0.2	0.0
LAC_{glass}	59.0	21.4	2.5	0.3	1.1	9.4	5.5	0.3	0.4	0.1
ETN_{glass}	47.7	17.4	11.2	5.2	10.4	3.6	2.0	1.7	0.2	0.6
KIL_{glass}	50.6	13.1	12.1	7.9	10.7	2.2	0.4	2.4	0.2	0.2

[a]Sample codes are listed in Table 1.

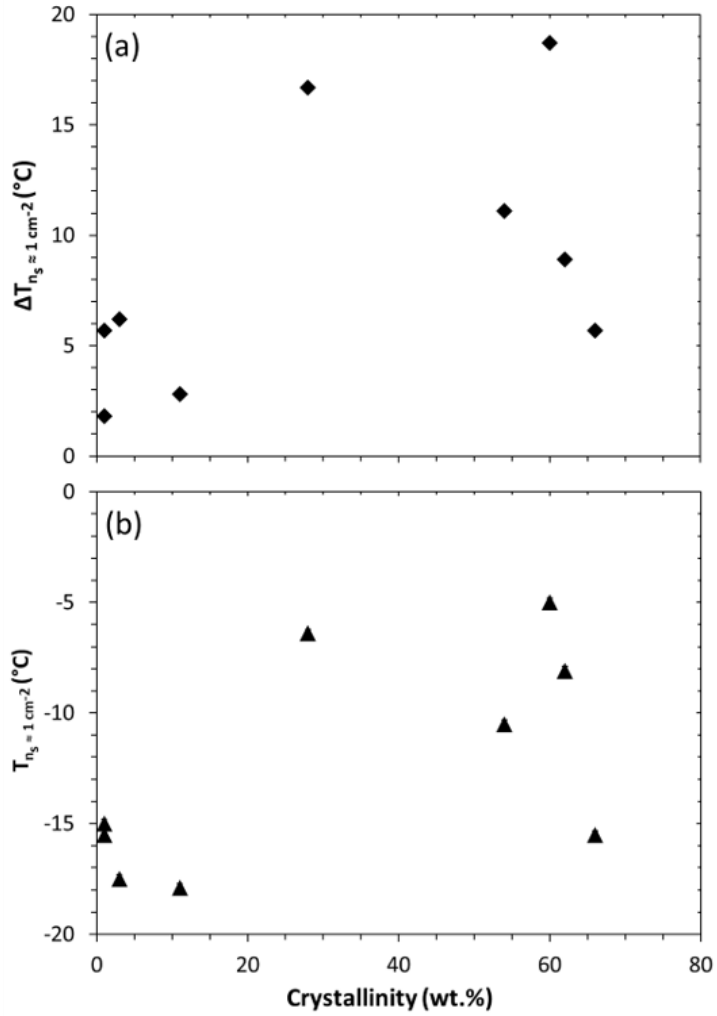

Figure S1. (a) The difference in IN~~E~~A ($\Delta T_{n_s \approx 1\ cm^{-2}}$) between the tephra and glass in each pair versus the crystallinity of the tephra, and (b) the IN~~E~~A ($T_{n_s \approx 1\ cm^{-2}}$) of the tephra versus the crystallinity of the tephra. Note that crystallinity below the XRD ~~detection~~quantification limit (LIP_{teph}, CID_{teph}) is plotted at 1 wt.%. Ice nucleation experiments were conducted with 1 wt.% suspensions of tephra or glass in water. The uncertainty in $T_{n_s \approx 1\ cm^{-2}}$ is shown as error bars (note that these are obscured by the data symbols).

Text S1. Electron microprobe analysis of the tephra samples was performed using a Cameca SX-100 instrument equipped with a LaB_6 cathode. ~~With respect to the beam sensitivity of glassy tephra samples, a~~A 10 µm ~~de~~focused beam was used at an accelerating voltage of 15 keV and a current of 5 nA to analyse at least five points for each crystalline phase in the tephra samples. Calibration was done on the following standard materials: albite - Na, Si; periclase - Mg; orthoclase - K, Al; wollastonite - Ca, Si; Fe_2O_3 - Fe; Cr_2O_3 - Cr; ilmenite - Ti; bustamite - Mn; apatite - P; vanadinite - Cl; anhydrite - S. Elemental detection limits in parts per million are as follows: Si - 786, Al - 655, Fe - 1573, Mg - 501, Ca - 747, Na - 973, K - 711, Ti - 894, Mn - 1401, P - 568, Cr - 1286, S - 767, Cl - 955.

Table S2. Average c~~C~~hemical composition of feldspar in tephra samples used in this study, determined by electron microprobe analysis and expressed in wt.%.

Sample[a]		**SiO_2**	**Al_2O_3**	**Fe_2O_3**	**MgO**	**CaO**	**Na_2O**	**K_2O**	**TiO_2**	**MnO**	**P_2O_5**	**Cr_2O_3**	**SO_3**	**Cl**	**Total**	**Na_2O/CaO in *pl***	**K_2O/Na_2O in *al***
COL_{teph}	*pl*	54.2	28.1	0.76	0.05	10.8	5.6	0.22	~~0.06~~< d.l.	~~0.04~~<d. l.	~~0.02~~< d.l.	-	-	-	99.7	0.5	-
TUN_{teph}	*pl*	55.7	27.4	1.1	0.10	10.9	5.3	0.44	0.09	~~0.01~~<d. l.	~~0.05~~< d.l.	~~0.08~~<d. l.	~~0.02~~< d.l.	~~0.02~~< d.l.	101.~~0~~2	0.5	-
AST_{teph}	*pl*	54.6	26.9	0.68	~~0.02~~< d.l.	9.6	4.7	2.5	0.04	~~0.02~~<d. l.	~~0.02~~< d.l.	~~0.01~~<d. l.	-	~~0.01~~< d.l.	99.~~0~~1	0.5	-
	al	63.7	19.3	0.40	~~0.01~~< d.l.	0.84	2.5	12.4	0.10	~~0.02~~<d. l.	-	~~0.03~~<d. l.	~~0.04~~< d.l.	-	99.~~2~~4	-	5.0
NUO_{teph}	*al*	64.0	20.7	0.85	~~0.04~~< d.l.	2.1	5.9	7.0	0.16	~~0.07~~<d. l.	~~0.03~~< d.l.	~~0.04~~<d. l.	~~0.01~~< d.l.	~~0.09~~< d.l.	10~~0~~1.7 ~~0~~	-	1.2
LAC_{teph}	*al*	63.9	20.2	0.76	0.05	1.3	4.8	9.2	0.14	~~0.03~~<d. l.	~~0.05~~< d.l.	~~0.02~~<d. l.	~~0.06~~< d.l.	~~0.06~~< d.l.	100.4	-	1.9
ETN_{teph}	*pl*	48.5	32.4	1.2	0.08	15.9	2.5	0.22	0.09	~~0.02~~<d. l.	~~0.04~~< d.l.	~~0.01~~<d. l.	~~0.02~~< d.l.	-	100.9	0.2	-
KIL_{teph}	*pl*	50.3	31.0	1.0	0.17	15.4	3.0	0.12	0.11	-	~~0.01~~< d.l.	-	~~0.07~~< d.l.	-	101.1~~2~~	0.2	-

[a]Sample codes are listed in Table 1. *pl* = plagioclase (Na-/Ca-) feldspar, *al* = alkali (K-) feldspar. d.l. = detection limit.

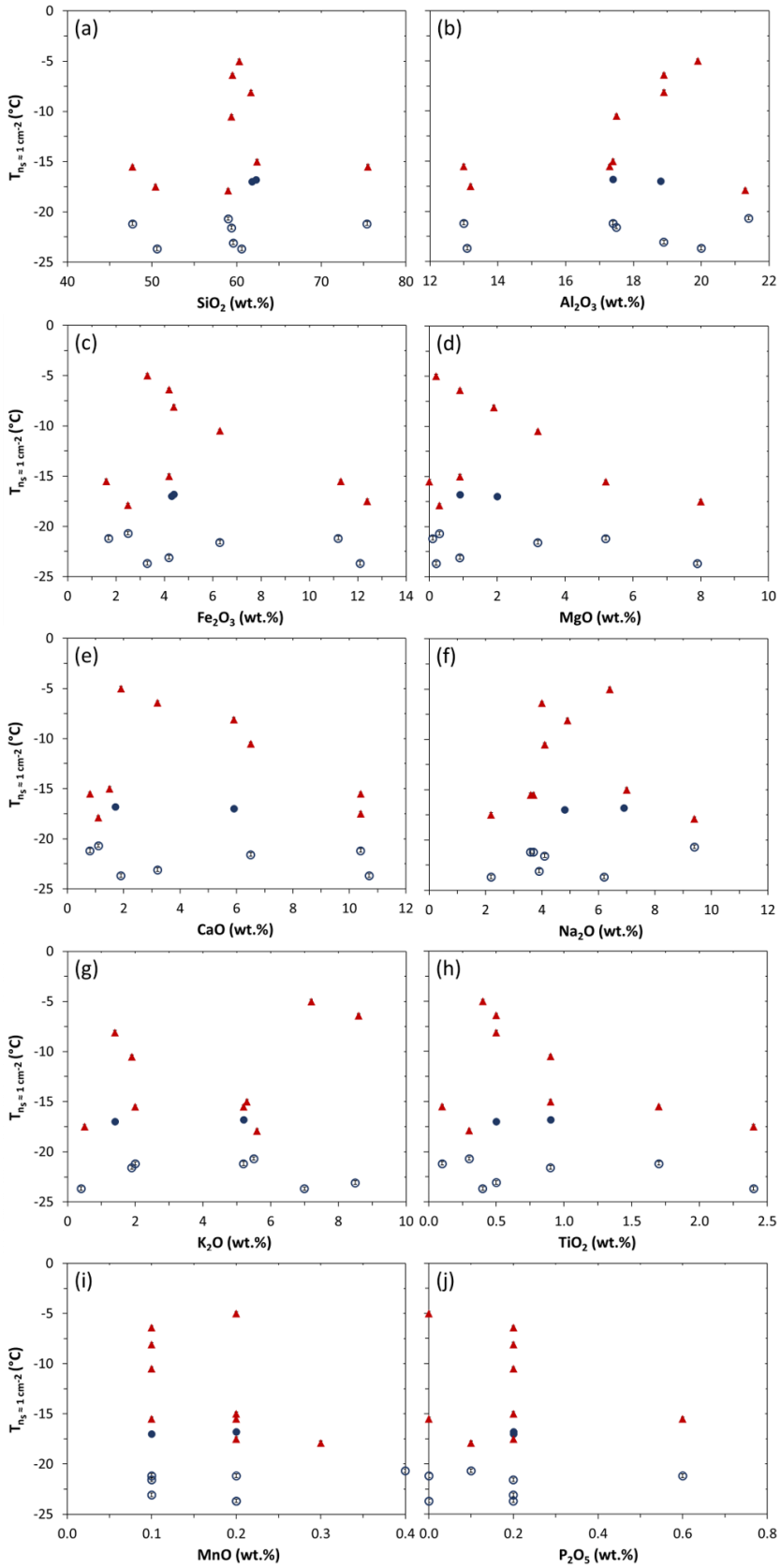

Figure S2. The IN~~E~~A ($T_{n_s \approx 1\ cm^{-2}}$) of the tephra (red triangles) and glass (blue circles) versus their (a) SiO_2, (b) Al_2O_3, (c) Fe_2O_3, (d) MgO, (e) CaO, (f) Na_2O, (g) K_2O, (h) TiO_2, (i) MnO, and (j) P_2O_5 contents. The open blue circles correspond to glasses (all except CID_{glass} and COL_{glass}) for which ice nucleation cannot be distinguished from that induced by the background water. Ice nucleation experiments were conducted with 1 wt.% suspensions of tephra or glass in water. The uncertainty in $T_{n_s \approx 1\ cm^{-2}}$ is shown as error bars (note that these are obscured by the data symbols).